

In this paper, we show that the monomial basis is generally as good as a well-conditioned polynomial basis for interpolation, provided that the condition number of the Vandermonde matrix is smaller than the reciprocal of machine epsilon. This leads to a practical algorithm for piecewise polynomial interpolation over general regions in the complex plane using the monomial basis. Our analysis also yields a new upper bound for the condition number of an arbitrary Vandermonde matrix, which generalizes several previous results.

**Keywords:** polynomial interpolation; monomials; Vandermonde matrix; backward error analysis

## On polynomial interpolation in the monomial basis

Zewen Shen<sup>† $\diamond$ \*</sup> and Kirill Serkh<sup>‡ $\diamond$</sup>   
v6, Dec 13, 2024

$\diamond$  This author's work was supported in part by the NSERC Discovery Grants RGPIN-2020-06022 and DGEER-2020-00356.

<sup>†</sup> Dept. of Computer Science, University of Toronto, Toronto, ON M5S 2E4

<sup>‡</sup> Dept. of Math. and Computer Science, University of Toronto, Toronto, ON M5S 2E4

\* Corresponding author

# Contents

<b>1</b>	<b>Introduction</b>	<b>2</b>
<b>2</b>	<b>Polynomial interpolation in the monomial basis</b>	<b>6</b>
2.1	Under what conditions is interpolation in the monomial basis as good as interpolation in a well-conditioned polynomial basis? . . . . .	14
2.2	Practical use of a monomial basis for interpolation . . . . .	16
<b>3</b>	<b>Numerical experiments</b>	<b>18</b>
3.1	Interpolation over an interval . . . . .	18
3.2	Approximation over more general regions in the complex plane . . . . .	19
<b>4</b>	<b>Applications</b>	<b>23</b>
4.1	Oscillatory integrals and singular integrals . . . . .	27
4.2	Root finding . . . . .	27
<b>5</b>	<b>Discussion</b>	<b>28</b>
<b>6</b>	<b>Acknowledgements</b>	<b>28</b>

## 1 Introduction

Function approximation has been a central topic in numerical analysis since its inception. One of the most effective methods for approximating a function  $F : [-1, 1] \rightarrow \mathbb{R}$  is the use of an interpolating polynomial  $P_N$  of degree  $N$  which satisfies  $P_N(x_j) = F(x_j)$  for a set of  $(N + 1)$  interpolation points  $\{x_j\}_{j=0,1,\dots,N}$ . In practice, the interpolation points are typically chosen to be the Chebyshev points, and the resulting interpolating polynomial, known as the Chebyshev interpolant, is a nearly optimal approximation to  $F$  in the space of polynomials of degree at most  $N$  [32]. A common basis for representing the interpolating polynomial  $P_N$  is the Lagrange polynomial basis, and the evaluation of  $P_N$  in this basis can be done stably using the Barycentric interpolation formula [9, 22]. Some other commonly used bases are Newton polynomials, Chebyshev polynomials, and Legendre polynomials. Alternatively, the monomial basis can be used to represent  $P_N$ , such that  $P_N(x) = \sum_{k=0}^N a_k x^k$  for some coefficients  $\{a_k\}_{k=0,1,\dots,N}$ . The computation of the monomial coefficient vector  $a^{(N)} := (a_0, a_1, \dots, a_N)^T \in \mathbb{R}^{N+1}$  of the interpolating polynomial  $P_N$  requires the solution of the linear system  $V^{(N)} a^{(N)} = f^{(N)}$ , where

$$V^{(N)} := \begin{pmatrix} 1 & x_0 & x_0^2 & \cdots & x_0^N \\ 1 & x_1 & x_1^2 & \cdots & x_1^N \\ \vdots & \vdots & \vdots & \ddots & \vdots \\ 1 & x_N & x_N^2 & \cdots & x_N^N \end{pmatrix} \in \mathbb{R}^{(N+1) \times (N+1)} \quad (1)$$

is a Vandermonde matrix, and  $f^{(N)} := (F(x_0), F(x_1), \dots, F(x_N))^T \in \mathbb{R}^{N+1}$  is a vector of the function values of  $F$  at the  $(N + 1)$  interpolation points on the interval  $[-1, 1]$ . It is well-known that, given any set of real interpolation points within the unit interval, the condition number of  $V^{(N)}$  grows at least as fast as  $\sqrt{2}(1 + \sqrt{2})^{N-1}/\sqrt{N+1}$  [8]. It follows that the accuracy of the numerical solution to this linear system deteriorates rapidly as  $N$  increases, and, as a result, this algorithm for constructing  $P_N$  is often

considered unstable. But, is this really the case? Let  $\{x_j\}_{j=0,1,\dots,N}$  be the set of  $(N+1)$  Chebyshev points on the interval  $[-1, 1]$ , and suppose that  $F(x) = \cos(2x + 1)$ . We solve the resulting Vandermonde system using LU factorization with partial pivoting. In Figure 1a, we show the polynomial interpolation error  $\|F - P_N\|_{L^\infty([-1,1])}$  and the monomial approximation error  $\|F - \hat{P}_N\|_{L^\infty([-1,1])}$ , where  $P_N$  is approximated using the Barycentric interpolation formula and  $\hat{P}_N$  is evaluated using the computed monomial expansion. The Chebyshev interpolant constructed from the computed monomial expansion is, surprisingly, as accurate as the Chebyshev interpolant evaluated using the Barycentric interpolation formula (which is accurate up to machine precision), despite the huge condition number of the Vandermonde matrix reported in Figure 1b.

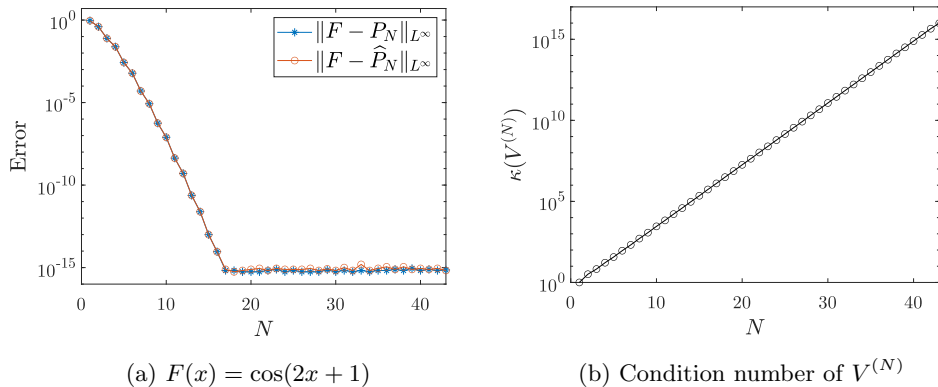
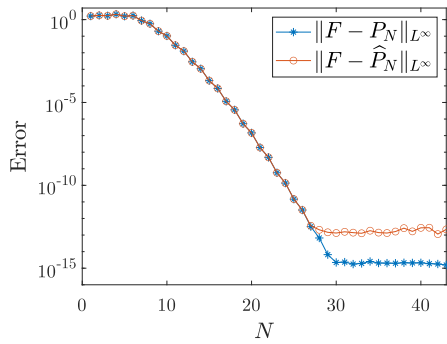


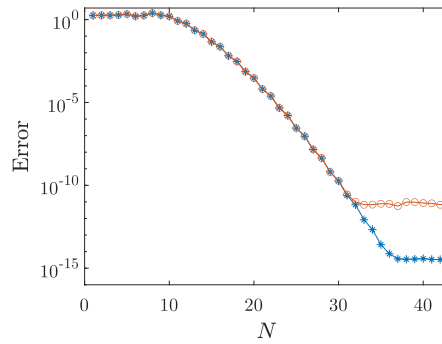
Figure 1: **Polynomial interpolation of  $\cos(2x + 1)$  in the monomial basis over  $[-1, 1]$ .** The  $x$ -axis label  $N$  denotes the order of approximation. The polynomial  $P_N$  denotes the interpolating polynomial approximated using the Barycentric interpolation formula. The polynomial  $\hat{P}_N$  denotes the computed monomial expansion. The  $L^\infty$  error is estimated by comparing the approximated function values at 10000 equidistant points over  $[-1, 1]$  with the true function values.

What happens when the function  $F$  requires a higher-order polynomial for accurate approximation? In Figure 2, we compare the accuracy of the two approximations when  $F(x) = \cos(8x + 1)$  and when  $F(x) = \cos(12x + 1)$ . Initially, the computed monomial expansion is as accurate as the Chebyshev interpolant evaluated using the Barycentric interpolation formula. However, the convergence of polynomial interpolation in the monomial basis stagnates after reaching a certain error threshold. It appears that, the higher the polynomial order necessary to approximate the functions, the larger that error threshold becomes. But consider the accuracy of the two approximations when  $F(x) = \frac{1}{x-\sqrt{2}}$  and when  $F(x) = \frac{1}{x-0.5i}$ , shown in Figure 3. These two functions each have a singularity in a neighborhood of the interval  $[-1, 1]$ , and Chebyshev interpolants of degree  $\geq 40$  are required to approximate them to machine precision. Yet, no stagnation of convergence is observed. In Figure 4, we consider the case where  $F$  is a non-smooth function, and we find that the accuracy of the two approximations is, once again, the same. The stability of polynomial interpolation in the monomial basis clearly depends in a subtle way on the function being approximated.

These seemingly mysterious experiments can be explained partially from the point of view of backward error analysis. The forward error  $\|a^{(N)} - \hat{a}^{(N)}\|_2$  of the numerical solution  $\hat{a}^{(N)}$  to the Vandermonde system  $V^{(N)}a^{(N)} = f^{(N)}$  can indeed be huge, but

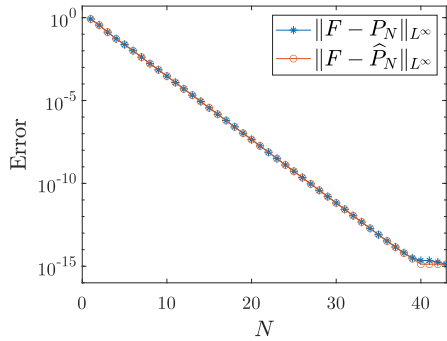


(a)  $F(x) = \cos(8x + 1)$

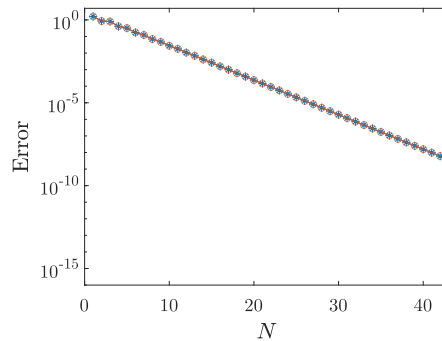


(b)  $F(x) = \cos(12x + 1)$

Figure 2: **Polynomial interpolation of more complicated functions in the monomial basis, over  $[-1, 1]$ .**



(a)  $F(x) = \frac{1}{x - \sqrt{2}}$



(b)  $F(x) = \frac{1}{x - 0.5i}$

Figure 3: **Polynomial interpolation of functions with a singularity near the approximation domain, in the monomial basis, over  $[-1, 1]$ .**

it is the backward error, i.e.,  $\|V^{(N)}\hat{a}^{(N)} - f^{(N)}\|_2$ , that matters for the accuracy of the approximation. This is because a backward error of size around machine precision implies that the difference between the computed monomial expansion, which we denote by  $\hat{P}_N$ , and the exact interpolating polynomial,  $P_N$ , is a polynomial which approximately vanishes at all of the interpolation points. More specifically, the residual error  $\|P_N - \hat{P}_N\|_{L^\infty([-1,1])}$  is bounded by  $\Lambda_N \cdot \|V^{(N)}\hat{a}^{(N)} - f^{(N)}\|_2$ , where  $\Lambda_N$  denotes the Lebesgue constant associated with the interpolation points. This constant is defined by the formula  $\Lambda_N = \sup_{F \in C([-1,1]), F \neq 0} \frac{\|P_N\|_\infty}{\|F\|_\infty}$ , with  $\|\cdot\|_\infty$  denoting the  $\infty$ -norm in  $C([-1,1])$ , and  $P_N$  denoting the interpolating polynomial of  $F$  for the given interpolation points. This constant grows logarithmically when well-conditioned interpolation points, such as Chebyshev points, are used. As a result, we can bound

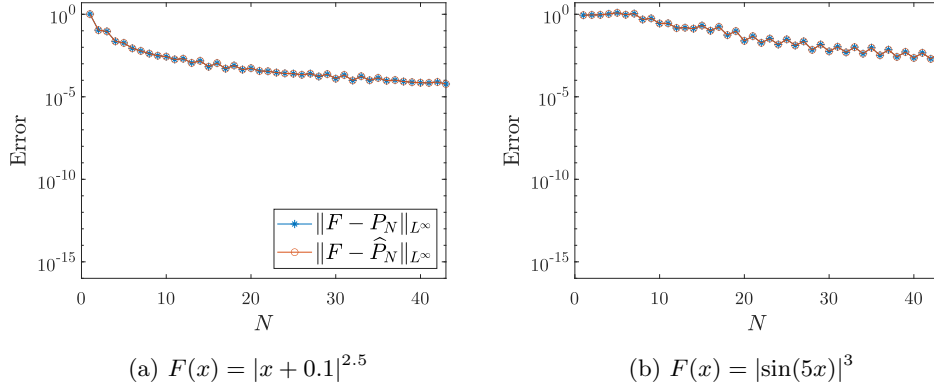


Figure 4: **Polynomial interpolation of non-smooth functions in the monomial basis, over  $[-1, 1]$ .**

the monomial approximation error  $\|F - \widehat{P}_N\|_{L^\infty([-1,1])}$  using the following inequality:

$$\begin{aligned}
\|F - \widehat{P}_N\|_{L^\infty([-1,1])} &\leq \|F - P_N\|_{L^\infty([-1,1])} + \|P_N - \widehat{P}_N\|_{L^\infty([-1,1])} \\
&\leq \|F - P_N\|_{L^\infty([-1,1])} + \Lambda_N \cdot \|V^{(N)}\widehat{a}^{(N)} - f^{(N)}\|_2 \\
&\lesssim \|F - P_N\|_{L^\infty([-1,1])} + \|V^{(N)}\widehat{a}^{(N)} - f^{(N)}\|_2. \tag{2}
\end{aligned}$$

Here, we introduce the notation  $x_N \lesssim y_N$  to indicate the existence of a constant  $c_N > 0$ , independent of the specific values of  $x_N$  and  $y_N$  but dependent on  $N$ , such that  $x_N \leq c_N y_N$ . This constant  $c_N$  is assumed to be a rational function of  $N$ , where  $N$  represents either the dimensionality or the approximation order. Additionally, we write  $x_N \approx y_N$  to mean that both  $x_N \lesssim y_N$  and  $y_N \lesssim x_N$ .

When the backward error is smaller than the polynomial interpolation error, the monomial approximation error is dominated by the polynomial interpolation error, and the use of a monomial basis does not incur any additional loss of accuracy. Once the polynomial interpolation error becomes smaller than the backward error, the convergence of the approximation stagnates. For example, for the function approximated in Figure 3a, we find that the backward error is around the size of machine epsilon for all  $N \leq 43$ , which explains why no stagnation is observed. On the other hand, in Figure 2a, the backward error is around the size of  $10^{-13}$  for  $N \geq 20$ , which leads to stagnation once the polynomial interpolation error is less than  $10^{-13}$ .

The explanation above brings up a new question: when will the backward error be small? Given a matrix  $A \in \mathbb{C}^{n \times n}$  and a vector  $b \in \mathbb{C}^n$ , the numerical solution  $\widehat{x}$  to the linear system  $Ax = b$  computed by a backward stable solver is the exact solution to the linear system

$$(A + \delta A)\widehat{x} = b \tag{3}$$

for a perturbation matrix  $\delta A \in \mathbb{C}^{n \times n}$  that satisfies  $\|\delta A\|_2 \leq u \cdot \zeta_n \|A\|_2$ , where  $u$  denotes machine epsilon and  $\zeta_n > 0$  is a small growth factor that is independent of  $A$  and  $b$  (see Section 7.6 in [21]). A classical example of a backward stable linear system solver is the Householder QR factorization, whose growth factor  $\zeta_n$  is bounded by a low-degree polynomial in  $n$  (see Theorem 19.5 and Equation (19.14) in [21]). Another commonly used solver, LU factorization with partial pivoting, has a growth factor  $\zeta_n$

that can grow exponentially as  $n$  increases (see Section 9.3 in [21]). This upper bound for  $\|\delta A\|_2$  is, however, rarely approached, and the stability of LU factorization with partial pivoting is often comparable to that of QR factorization in practice (see Lecture 22 in [34] for a detailed discussion). When we state in this paper that a linear system is solved using a backward stable solver, we assume that the growth factor  $\zeta_n$  associated with this solver is bounded by a low-degree polynomial in  $n$  with small coefficients.

When the Vandermonde system  $V^{(N)}a^{(N)} = f^{(N)}$  is solved using a backward stable solver, the backward error of the numerical solution to the Vandermonde system satisfies  $\|V^{(N)}\hat{a}^{(N)} - f^{(N)}\|_2 = \|\delta V^{(N)}\hat{a}^{(N)}\|_2 \leq u \cdot \zeta_n \|V^{(N)}\|_2 \|\hat{a}^{(N)}\|_2$ . Since  $\|V^{(N)}\|_2 \in [\sqrt{N+1}, N+1]$  when the interpolation points are inside the unit interval  $[-1, 1]$ , the backward error is essentially dominated by  $u \cdot \|\hat{a}^{(N)}\|_2$ . Furthermore, one can show that  $\|\hat{a}^{(N)}\|_2 \approx \|a^{(N)}\|_2$  when the condition number of  $V^{(N)}$  satisfies  $\kappa(V^{(N)}) \lesssim \frac{1}{u}$  (see Theorem 2.2 for a formal statement). It follows that the monomial approximation error can be quantified a priori using information about the interpolating polynomial, which means that a theory of polynomial interpolation in the monomial basis can be developed. Although the examples provided in this section are limited to the interval  $[-1, 1]$ , it is important to note that these observations are equally applicable to a simply connected compact domain in the complex plane. In the rest of the paper, we consider polynomial interpolation in the monomial basis over a simply connected compact domain in the complex plane, with the interval as a special case.

The rest of the paper is organized as follows. In Section 2, we analyze polynomial interpolation in the monomial basis over a simply connected compact domain in the complex plane. Our analysis reveals the conditions under which the monomial basis is as good as a well-conditioned polynomial basis for interpolation, resulting in a practical algorithm for using the monomial basis, with no extra error and with almost no extra cost. As a by-product of our analysis, we derive a tight upper bound for the condition number of any Vandermonde matrix (see Theorem 2.5). In Section 3, we provide extensive numerical experiments to support our analysis. In Section 4, we present applications where the use of a monomial basis for interpolation offers a substantial advantage over other bases. In Section 5, we summarize our key points, review related work, and discuss generalizations of our results.

## 2 Polynomial interpolation in the monomial basis

In this section, we consider polynomial interpolation of a function over a simply connected compact set in the complex plane. We structure the section as follows. First, we show in Theorem 2.2 that, when  $\kappa(V^{(N)}) \lesssim \frac{1}{u}$ , the monomial approximation error is bounded by the sum of the polynomial interpolation error and an extra error term that involves the 2-norm of the monomial coefficient vector of the interpolant. Then, we provide tight upper bounds for this extra error term and for the growth of the condition number of the Vandermonde matrix in Theorems 2.4 and 2.5, respectively. In Section 2.1, we elucidate the frequently observed and seemingly paradoxical success of polynomial interpolation in the monomial basis when  $\kappa(V^{(N)}) \lesssim \frac{1}{u}$ . Finally, we summarize the necessary considerations for the proper usage of the monomial basis in Section 2.2.

Let  $\Omega \subset \mathbb{C}$  be simply connected and compact, and let  $F : \Omega \rightarrow \mathbb{C}$  be an arbitrary function. The  $N$ th degree interpolating polynomial, denoted by  $P_N$ , of the function  $F$  for a given set of  $(N+1)$  distinct interpolation points  $Z := \{z_j\}_{j=0,1,\dots,N} \subset \Omega$  can be expressed as  $P_N(z) = \sum_{k=0}^N a_k z^k$ , where the monomial coefficient vector

$(a_0, a_1, \dots, a_N)^T$  is the solution to the Vandermonde system

$$\begin{pmatrix} 1 & z_0 & z_0^2 & \cdots & z_0^N \\ 1 & z_1 & z_1^2 & \cdots & z_1^N \\ \vdots & \vdots & \vdots & \ddots & \vdots \\ 1 & z_N & z_N^2 & \cdots & z_N^N \end{pmatrix} \begin{pmatrix} a_0 \\ a_1 \\ \vdots \\ a_N \end{pmatrix} = \begin{pmatrix} F(z_0) \\ F(z_1) \\ \vdots \\ F(z_N) \end{pmatrix}. \quad (4)$$

In this paper, we choose to fix the set of basis functions as  $\{z^k\}_{k=0,1,\dots,N}$ . However, depending on the geometry and location of  $\Omega$ , it can be advantageous to use a scaled and translated monomial basis  $\{(\frac{z-\mu}{\nu})^k\}_{k=0,1,\dots,N}$ . Our analysis also encompasses this case, as the Vandermonde system corresponding to the scaled and translated basis with the points  $\{z_j\}_{j=0,1,\dots,N} \subset \Omega$  is equivalent to that of the original basis  $\{z^k\}_{k=0,1,\dots,N}$  using the transformed points  $\{\frac{z_j-\mu}{\nu}\}_{j=0,1,\dots,N} \subset \frac{\Omega-\mu}{\nu}$ . We assume without loss of generality that  $\Omega$  lies within the unit disk, ensuring that  $\|V^{(N)}\|_2 \in [\sqrt{N+1}, N+1]$ .

In the following, we denote the Vandermonde matrix, the monomial coefficient vector, and the right-hand side vector by  $V^{(N)}$ ,  $a^{(N)}$ , and  $f^{(N)}$ , respectively.

In order to study the size of the residual of the numerical solution to the Vandermonde system, we require the following lemma, which provides a bound for the 2-norm of the solution to a perturbed linear system.

**Lemma 2.1.** *Let  $N$  be a positive integer. Suppose that  $A \in \mathbb{C}^{N \times N}$  is invertible,  $b \in \mathbb{C}^N$ , and that  $x \in \mathbb{C}^N$  satisfies  $Ax = b$ . Suppose further that  $\hat{x} \in \mathbb{C}^N$  satisfies  $(A + \delta A)\hat{x} = b$  for some  $\delta A \in \mathbb{C}^{N \times N}$ . If there exists an  $\alpha > 1$  such that*

$$\|\delta A\|_2 \leq \frac{1}{\alpha \cdot \|A^{-1}\|_2}, \quad (5)$$

then the matrix  $A + \delta A$  is invertible, and  $\hat{x}$  satisfies

$$\frac{\alpha}{\alpha + 1} \|x\|_2 \leq \|\hat{x}\|_2 \leq \frac{\alpha}{\alpha - 1} \|x\|_2. \quad (6)$$

**Proof.** By multiplying both sides of  $(A + \delta A)\hat{x} = b$  by  $A^{-1}$ , we have that

$$(I + A^{-1}\delta A)\hat{x} = x, \quad (7)$$

where  $I$  denotes the identity matrix. By (5), the term  $A^{-1}\delta A$  satisfies

$$\|A^{-1}\delta A\|_2 \leq \|A^{-1}\|_2 \|\delta A\|_2 \leq \frac{1}{\alpha} < 1. \quad (8)$$

Thus, it follows that the matrix  $A + \delta A$  is invertible, and  $\|\hat{x}\|_2$  satisfies

$$\|\hat{x}\|_2 \leq \|(I + A^{-1}\delta A)^{-1}\|_2 \|x\|_2 \leq \frac{1}{1 - \|A^{-1}\delta A\|_2} \|x\|_2 \leq \frac{\alpha}{\alpha - 1} \|x\|_2. \quad (9)$$

In addition, by (8),  $\|x\|_2$  satisfies

$$\|x\|_2 \leq \|I + A^{-1}\delta A\|_2 \|\hat{x}\|_2 \leq \left(1 + \frac{1}{\alpha}\right) \|\hat{x}\|_2. \quad (10)$$

The proof is completed by combining (9) and (10). ■

The following theorem provides upper bounds for the monomial approximation error. It is related to frame approximation [3, 4] and the method of fundamental solutions [6, 31] in the sense that it also uses a similar idea, that it is possible to achieve a small approximation error with an ill-conditioned basis, provided that there exists a small coefficient vector with a good fit.

**Theorem 2.2.** *Suppose that there exists some constant  $\gamma_N \geq 0$  such that the computed monomial coefficient vector  $\widehat{a}^{(N)} = (\widehat{a}_0, \widehat{a}_1, \dots, \widehat{a}_N)^T$  satisfies*

$$(V^{(N)} + \delta V^{(N)})\widehat{a}^{(N)} = f^{(N)} \quad (11)$$

for some  $\delta V^{(N)} \in \mathbb{C}^{(N+1) \times (N+1)}$  with

$$\|\delta V^{(N)}\|_2 \leq u \cdot \gamma_N, \quad (12)$$

where  $u$  denotes machine epsilon. Let  $\widehat{P}_N(z) := \sum_{k=0}^N \widehat{a}_k z^k$  be the computed monomial expansion. The monomial approximation error is bounded by

$$\|F - \widehat{P}_N\|_{L^\infty(\Omega)} \leq \|F - P_N\|_{L^\infty(\Omega)} + u \cdot \gamma_N \Lambda_N \|\widehat{a}^{(N)}\|_2, \quad (13)$$

where  $\Lambda_N := \sup_{F \in C(\Omega), F \neq 0} \frac{\|P_N\|_{L^\infty(\Omega)}}{\|F\|_{L^\infty(\Omega)}}$  is the Lebesgue constant for  $Z$ . If, in addition,

$$\|(V^{(N)})^{-1}\|_2 \leq \frac{1}{2u \cdot \gamma_N}, \quad (14)$$

then the 2-norm of the numerical solution  $\widehat{a}^{(N)}$  is bounded by

$$\frac{2}{3} \|a^{(N)}\|_2 \leq \|\widehat{a}^{(N)}\|_2 \leq 2 \|a^{(N)}\|_2, \quad (15)$$

and the monomial approximation error can be quantified a priori by

$$\|F - \widehat{P}_N\|_{L^\infty(\Omega)} \leq \|F - P_N\|_{L^\infty(\Omega)} + 2u \cdot \gamma_N \Lambda_N \|a^{(N)}\|_2. \quad (16)$$

**Proof.** By the triangle inequality, the definition of the Lebesgue constant  $\Lambda_N$ , equation (11) and inequality (12), the monomial approximation error satisfies

$$\begin{aligned} \|F - \widehat{P}_N\|_{L^\infty(\Omega)} &\leq \|F - P_N\|_{L^\infty(\Omega)} + \|\widehat{P}_N - P_N\|_{L^\infty(\Omega)} \\ &\leq \|F - P_N\|_{L^\infty(\Omega)} + \Lambda_N \|V^{(N)}\widehat{a}^{(N)} - f^{(N)}\|_2 \\ &\leq \|F - P_N\|_{L^\infty(\Omega)} + u \cdot \gamma_N \Lambda_N \|\widehat{a}^{(N)}\|_2. \end{aligned} \quad (17)$$

If  $\|(V^{(N)})^{-1}\|_2 \leq \frac{1}{2u \cdot \gamma_N}$ , then by Lemma 2.1, the 2-norm of the computed monomial coefficient vector  $\widehat{a}^{(N)}$  is bounded by

$$\frac{2}{3} \|a^{(N)}\|_2 \leq \|\widehat{a}^{(N)}\|_2 \leq 2 \|a^{(N)}\|_2, \quad (18)$$

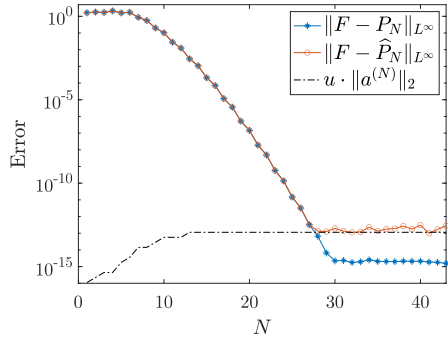
and (17) becomes

$$\|F - \widehat{P}_N\|_{L^\infty(\Omega)} \leq \|F - P_N\|_{L^\infty(\Omega)} + 2u \cdot \gamma_N \Lambda_N \|a^{(N)}\|_2. \quad (19)$$

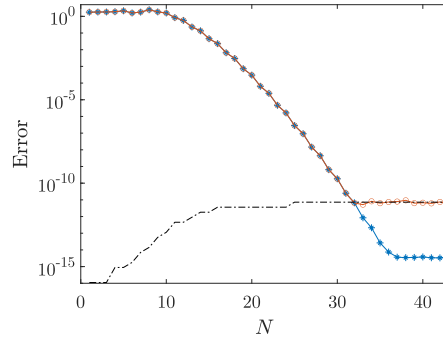
■

As described in the introduction, when the Vandermonde system is solved using a backward stable linear system solver, the set of assumptions (11) and (12) is satisfied with a constant  $\gamma_N \leq \zeta_N \|V^{(N)}\|_2$ , where  $\zeta_N > 0$  is a growth factor bounded by a low-degree polynomial in  $N$ , and is independent of the matrix and the right-hand-side vector. It follows then that  $\gamma_N \lesssim 1$ . Therefore, given interpolation points with a

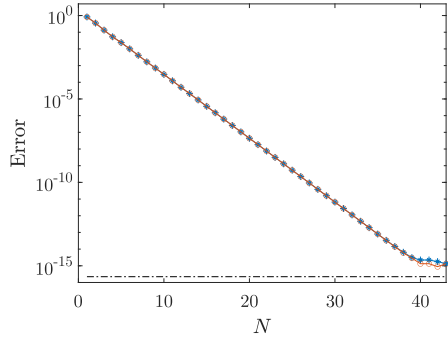




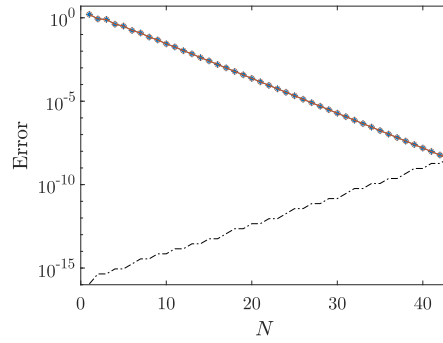
(a)  $F(x) = \cos(8x + 1)$



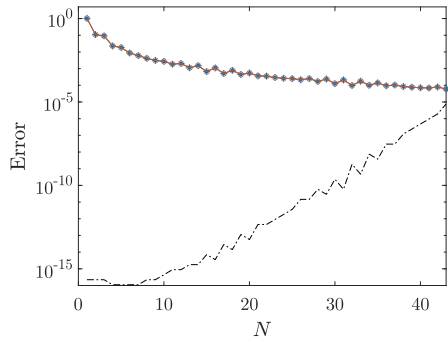
(b)  $F(x) = \cos(12x + 1)$



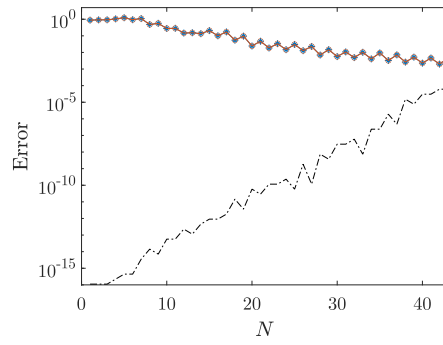
(c)  $F(x) = \frac{1}{x - \sqrt{2}}$



(d)  $F(x) = \frac{1}{x - 0.5i}$



(e)  $F(x) = |x + 0.1|^{2.5}$



(f)  $F(x) = |\sin(5x)|^3$

Figure 5: **Polynomial interpolation error, monomial approximation error and  $u \cdot \|a^{(N)}\|_2$ , for  $\Omega = [-1, 1]$ .** These functions are the ones that appear in Section 1.

Lebesgue constant  $\Lambda_N \lesssim 1$ , we have that  $\|F - \widehat{P}_N\|_{L^\infty(\Omega)} \lesssim \|F - P_N\|_{L^\infty(\Omega)} + u\|a^{(N)}\|_2$  when  $\kappa(V^{(N)}) \lesssim 1/u$ , where we write the condition (14) as  $\kappa(V^{(N)}) = \|V^{(N)}\|_2 \cdot \|(V^{(N)})^{-1}\|_2 \leq \frac{\|V^{(N)}\|_2}{2u \cdot \gamma_N} \lesssim 1/u$ . In Figure 5, we plot the values of  $\|F - \widehat{P}_N\|_{L^\infty(\Omega)}$ ,  $\|F - P_N\|_{L^\infty(\Omega)}$ , and  $u\|a^{(N)}\|_2$ , for the functions appearing in Section 1, in order to validate the theorem above.

**Remark 2.1.** The second term on the right-hand side of (16) is an upper bound of the backward error  $\|P_N - \widehat{P}_N\|_{L^\infty(\Omega)}$ , i.e., the extra loss of accuracy caused by the use of a monomial basis. Note that the absolute condition number of the evaluation of  $P_N(z)$  in the monomial basis is  $\lesssim \|a^{(N)}\|_2$  when  $|z| \approx 1$ , so that the resulting error is  $\lesssim u \cdot \|a^{(N)}\|_2$ , which is around the same size as  $2u \cdot \gamma_N \Lambda_N \|a^{(N)}\|_2$ .

**Remark 2.2.** It is well-known that selecting a set of interpolation points with a small Lebesgue constant is crucial for the interpolating polynomial  $P_N$  to approximate the function  $F$  nearly as accurately as the optimal polynomial approximant [32]. This requirement on the Lebesgue constant  $\Lambda_N$  of the interpolation points, that  $\Lambda_N \lesssim 1$ , can be circumvented by instead constructing an approximating polynomial using least-squares fitting. To construct such an approximating polynomial, one typically selects sample points on the boundary of the domain and uses a polynomial basis whose dimension is smaller than the number of sample points, as in, for example, [33]. Although our theoretical analysis only addresses approximations constructed using interpolation, the analysis for the least-squares case bears considerable similarity. The principal difference lies in the requirement for a more general notion of the Lebesgue constant. One such idea, using the 2-norm of the pseudoinverse mapping values at the sample points to the coefficients of an expansion in a basis, appears in [37].

In order to determine the relationship between the size of the monomial coefficient vector and the properties of the function being approximated, we will need the following definition, which generalizes the Bernstein ellipse to the case of a simply connected compact set in the complex plane.

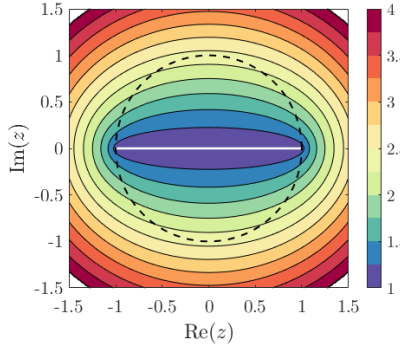
**Definition 2.1.** Given a simply connected compact set  $\Omega$  in the complex plane and  $\rho > 1$ , we define  $E_\rho$  to be the level set  $\{x+iy \in \mathbb{C} : G(x, y) = \log \rho\}$ , where  $G : \mathbb{R}^2 \rightarrow \mathbb{R}$  is the unique solution to the exterior Laplace equation

$$\begin{aligned} \nabla^2 G &= 0 \text{ in } \mathbb{R}^2 \setminus \Omega, \\ G &= 0 \text{ on } \partial\Omega, \\ G(x, y) &\sim \log r \text{ as } r := \sqrt{x^2 + y^2} \rightarrow \infty. \end{aligned} \tag{20}$$

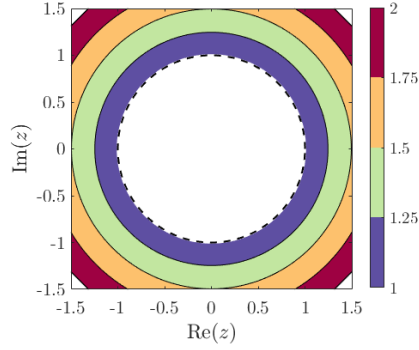
We let  $E_\rho^o$  denote the bounded open region with boundary  $E_\rho$ .

**Remark 2.3.** One can show that the function  $G$  defined above is positive in  $\mathbb{R}^2 \setminus \Omega$ . Given a harmonic conjugate  $H : \mathbb{R}^2 \setminus \Omega \rightarrow \mathbb{R}$  of  $G$ , the function  $\Phi(x+iy) := e^{G(x,y)+iH(x,y)}$  is a conformal mapping from  $\mathbb{C} \setminus \Omega$  to  $\mathbb{C} \setminus \overline{D}_1$ , where  $D_1$  is the open unit disk centered at the origin (see Section 4.1 in [35]). When  $\partial\Omega$  is continuous,  $\Phi^{-1}$  can be extended continuously from  $\mathbb{C} \setminus D_1$  to  $\mathbb{C} \setminus \Omega$  (see Section 2.1 in [27]). Furthermore, when  $\partial\Omega$  is a Jordan curve,  $\Phi$  becomes a continuous bijective map from  $\mathbb{C} \setminus D_1$  to  $\mathbb{C} \setminus \Omega$ .

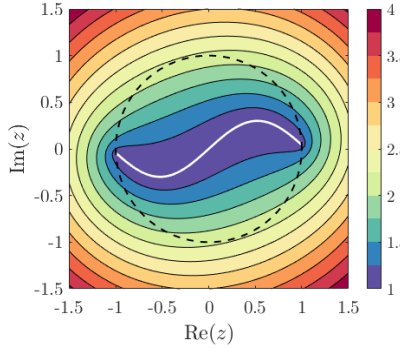
When  $\Omega = [a, b] \subset \mathbb{R}$ , the level set  $E_\rho$  is a Bernstein ellipse with parameter  $\rho$ , with foci at  $a$  and  $b$ . In Figure 6, we plot examples of level sets  $E_\rho$  for various sets  $\Omega$ , for different values of  $\rho$ .



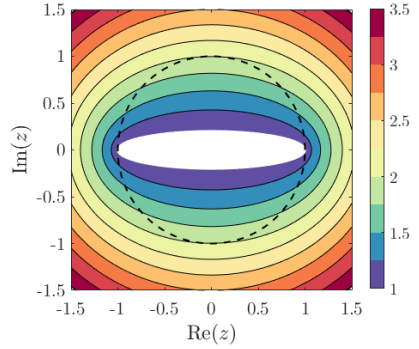
(a)  $\Omega = \{t : t \in [-1, 1]\}$



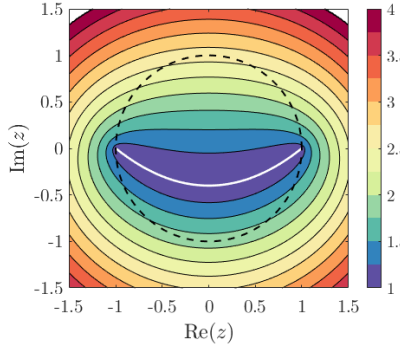
(b)  $\Omega = \{re^{\pi it} : r \in [0, 1], t \in [-1, 1]\}$



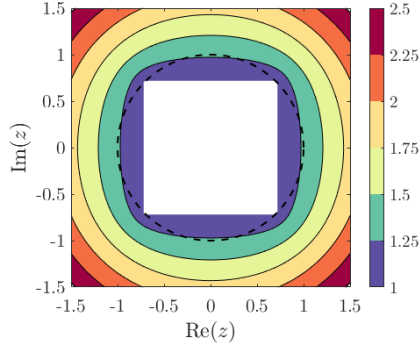
(c)  $\Omega = \{t + 0.3i \sin(3t) : t \in [-1, 1]\}$



(d)  $\Omega = \{r(\cos(\pi t) + 0.2i \sin(\pi t)) : r \in [0, 1], t \in [-1, 1]\}$



(e)  $\Omega = \{t + 0.4i(t^2 - 1) : t \in [-1, 1]\}$



(f)  $\Omega = \{a + bi : a, b \in [-\sqrt{2}/2, \sqrt{2}/2]\}$

Figure 6: **The level sets  $E_\rho$  for several values of  $\rho$ , corresponding to various sets  $\Omega$ .** The level sets  $E_\rho$  for  $\rho = 1, 1.25, 1.5, \dots$  appear as the boundaries between the colored regions in this figure. The color bar indicates which boundary corresponds to which value of  $\rho$ . The set  $\Omega$  is shown in white. The dashed circle is the boundary of the open unit disk, used in the definition of  $\rho_*$  in Definition 2.2. The plots were made using the source code provided in [2].

The parameter  $\rho_*$  defined below appears in our bounds for both the 2-norm of the monomial coefficient vector of the interpolating polynomial, and the growth rate of the 2-norm of the inverse of a Vandermonde matrix. It denotes the parameter of the smallest region  $E_\rho^o$  that contains the open unit disk centered at the origin.

**Definition 2.2.** Given a simply connected compact set  $\Omega \subset \mathbb{C}$ , we define  $\rho_* := \inf\{\rho > 1 : D_1 \subset E_\rho^o\}$ , where  $D_1$  is the open unit disk centered at the origin, and  $E_\rho^o$  is the region corresponding to  $\Omega$  defined in Definition 2.1.

The following lemma provides an upper bound for the 2-norm of the monomial coefficient vector of an arbitrary polynomial. We will use this lemma to prove a much tighter bound in Theorem 2.4.

**Lemma 2.3.** Let  $P_N : \mathbb{C} \rightarrow \mathbb{C}$  be a polynomial of degree  $N$ , where  $P_N(z) = \sum_{k=0}^N a_k z^k$  for some  $a_0, a_1, \dots, a_N \in \mathbb{C}$ . Let  $D_1$  denote the open unit disk centered at the origin, and suppose that  $\Omega \subset \mathbb{C}$  is simply connected and compact. The 2-norm of the coefficient vector  $a^{(N)} := (a_0, a_1, \dots, a_N)^T$  satisfies

$$\|a^{(N)}\|_2 \leq \|P_N\|_{L^\infty(\partial D_1)} \leq \rho_*^N \|P_N\|_{L^\infty(\Omega)}, \quad (21)$$

where  $\rho_*$  is given in Definition 2.2.

**Proof.** Observe that  $P_N(e^{i\theta}) = \sum_{k=0}^N a_k e^{ik\theta}$ . By Parseval's identity, we have that

$$\|a^{(N)}\|_2 = \left( \frac{1}{2\pi} \int_0^{2\pi} |P_N(e^{i\theta})|^2 d\theta \right)^{1/2} \leq \|P_N\|_{L^\infty(\partial D_1)} \leq \|P_N\|_{L^\infty(E_{\rho_*}^o)}, \quad (22)$$

where the last inequality comes from the fact that  $D_1 \subset E_{\rho_*}^o$  (see Definition 2.1). Finally, using one of Bernstein's inequalities (see Section 4.6 in [35]), we have that

$$\|P_N\|_{L^\infty(E_{\rho_*}^o)} \leq \rho_*^N \|P_N\|_{L^\infty(\Omega)}. \quad (23)$$

■

The following theorem is the principal result of this paper. It demonstrates that the upper bound for the 2-norm of the monomial coefficient vector of an arbitrary polynomial, provided in Lemma 2.3, can be significantly improved if the given polynomial is viewed as an interpolating polynomial of a function  $F$ . Instead of using only the size of  $\|P_N\|_{L^\infty(\Omega)}$ , this theorem uses the properties of the function  $F$ .

**Theorem 2.4.** Let  $\Omega$  be a simply connected compact set in the complex plane, and let  $F : \Omega \rightarrow \mathbb{C}$  be an arbitrary function. Suppose that there exists a finite sequence of polynomials  $\{Q_n\}_{n=0,1,\dots,N}$ , where  $Q_n$  has degree  $n$ , which satisfies

$$\|F - Q_n\|_{L^\infty(\Omega)} \leq C_N \rho^{-n}, \quad 0 \leq n \leq N, \quad (24)$$

for some constants  $\rho > 1$  and  $C_N \geq 0$ . Define  $P_N(z) = \sum_{k=0}^N a_k z^k$  to be the  $N$ th degree interpolating polynomial of  $F$  for a given set of distinct interpolation points  $Z = \{z_j\}_{j=0,1,\dots,N} \subset \Omega$ . The 2-norm of the monomial coefficient vector  $a^{(N)} := (a_0, a_1, \dots, a_N)^T$  of  $P_N$  satisfies

$$\|a^{(N)}\|_2 \leq \|F\|_{L^\infty(\Omega)} + C_N \left( \Lambda_N \left( \frac{\rho_*}{\rho} \right)^N + 2\rho_* \sum_{j=0}^{N-1} \left( \frac{\rho_*}{\rho} \right)^j + 1 \right), \quad (25)$$

where  $\rho_*$  is given in Definition 2.2, and  $\Lambda_N$  denotes the Lebesgue constant for  $Z$ .

**Proof.** Given  $n \geq 0$ , let  $M^{(n)} : \mathbb{C}^{n+1} \rightarrow \mathcal{P}_n$  be the bijective linear map associating each vector  $(u_0, u_1, \dots, u_n)^T \in \mathbb{R}^{n+1}$  with the  $n$ th degree polynomial  $\sum_{k=0}^n u_k z^k \in \mathcal{P}_n$ . It follows immediately from Lemma 2.3 that, given any polynomial  $P \in \mathcal{P}_n$ ,

$$\|(M^{(n)})^{-1}[P]\|_2 \leq \rho_*^n \|P\|_{L^\infty(\Omega)}. \quad (26)$$

Therefore, by the triangle inequality, the 2-norm of the monomial coefficient vector of the polynomial  $Q_N$  satisfies

$$\begin{aligned} \|(M^{(N)})^{-1}[Q_N]\|_2 &\leq \|(M^{(N)})^{-1}[Q_0]\|_2 + \sum_{j=0}^{N-1} \|(M^{(N)})^{-1}[Q_{j+1} - Q_j]\|_2 \\ &= \|Q_0\|_{L^\infty(\Omega)} + \sum_{j=0}^{N-1} \|(M^{(j+1)})^{-1}[Q_{j+1} - Q_j]\|_2 \\ &\leq (\|F\|_{L^\infty(\Omega)} + C_N) + \sum_{j=0}^{N-1} \rho_*^{j+1} \|Q_{j+1} - Q_j\|_{L^\infty(\Omega)} \\ &\leq (\|F\|_{L^\infty(\Omega)} + C_N) + 2C_N \rho_* \sum_{j=0}^{N-1} \left(\frac{\rho_*}{\rho}\right)^j, \end{aligned} \quad (27)$$

from which it follows that  $\|a^{(N)}\|_2$  satisfies

$$\begin{aligned} \|a^{(N)}\|_2 &\leq \|(M^{(N)})^{-1}[P_N - Q_N]\|_2 + \|(M^{(N)})^{-1}[Q_N]\|_2 \\ &\leq \rho_*^N \|P_N - Q_N\|_{L^\infty(\Omega)} + \|(M^{(N)})^{-1}[Q_N]\|_2 \\ &\leq \rho_*^N \Lambda_N \|F - Q_N\|_{L^\infty(\Omega)} + \|(M^{(N)})^{-1}[Q_N]\|_2 \\ &\leq \|F\|_{L^\infty(\Omega)} + C_N \left( \Lambda_N \left(\frac{\rho_*}{\rho}\right)^N + 2\rho_* \sum_{j=0}^{N-1} \left(\frac{\rho_*}{\rho}\right)^j + 1 \right), \end{aligned} \quad (28)$$

where the third inequality comes from the observation that  $P_N - Q_N$  is the interpolating polynomial of  $F - Q_N$  for the set of interpolation points  $Z$ .  $\blacksquare$

**Remark 2.4.** The assumption (24) made in Theorem 2.4 can be satisfied for any function  $F$  by choosing  $C_N$  to be sufficiently large. When the function  $F$  has, for some  $\rho > \rho_*$ , an analytic continuation on the closure of the region  $E_\rho^o$  corresponding to  $\Omega$  (see Definitions 2.1 and 2.2), one can show that  $\|a^{(N)}\|_2 \lesssim 2\|F\|_{L^\infty(\partial D_1)}$ , where  $D_1$  is the open unit disk centered at the origin. This result is derived from Section 4.7 in [35], which establishes that  $\|F - P_N\|_{L^\infty(E_{\rho_*}^o)} = \mathcal{O}((\rho_*/\rho)^N)$ , where the asymptotic constant is proportional to  $\|F\|_{L^\infty(E_{\rho_*}^o)}$ . Consequently, it follows that

$$\|a^{(N)}\|_2 \leq \|P_N\|_{L^\infty(\partial D_1)} \leq \|F - P_N\|_{L^\infty(\partial D_1)} + \|F\|_{L^\infty(\partial D_1)} \lesssim 2\|F\|_{L^\infty(\partial D_1)}. \quad (29)$$

Theorem 2.4 provides an a priori upper bound on the 2-norm of the monomial coefficient vector. In order to apply Theorem 2.2, we also need to determine when the condition  $\|(V^{(N)})^{-1}\|_2 \leq \frac{1}{2u \cdot \gamma_N}$  applies. The following theorem, which is an immediate corollary of Lemma 2.3, bounds the growth of  $\|(V^{(N)})^{-1}\|_2$ . It includes some previous results [14, 15] as special cases of our bound.

**Theorem 2.5.** Suppose that  $V^{(N)} \in \mathbb{C}^{(N+1) \times (N+1)}$  is a Vandermonde matrix with  $(N+1)$  distinct interpolation points  $Z = \{z_j\}_{j=0,1,\dots,N} \subset \mathbb{C}$ . Suppose further that  $\Omega \subset \mathbb{C}$  is a simply connected compact set such that  $Z \subset \Omega$ . The 2-norm of  $(V^{(N)})^{-1}$  is bounded by

$$\|(V^{(N)})^{-1}\|_2 \leq \rho_*^N \Lambda_N, \quad (30)$$

where  $\rho_*$  is given in Definition 2.2, and  $\Lambda_N$  denotes the Lebesgue constant for the set of interpolation points  $Z$  over  $\Omega$ .

**Proof.** Let  $f^{(N)} = (f_0, f_1, \dots, f_N)^T \in \mathbb{C}^{N+1}$  be an arbitrary vector. Suppose that  $P_N$  is an interpolating polynomial of degree  $N$  for the set  $\{(z_j, f_j)\}_{j=0,1,\dots,N}$ . By Lemma 2.3, the 2-norm of the monomial coefficient vector  $a^{(N)}$  of  $P_N$  satisfies

$$\|a^{(N)}\|_2 \leq \rho_*^N \|P_N\|_{L^\infty(\Omega)} \leq \rho_*^N \Lambda_N \|f^{(N)}\|_\infty \leq \rho_*^N \Lambda_N \|f^{(N)}\|_2, \quad (31)$$

where the second inequality follows from the definition of the Lebesgue constant. Therefore, the 2-norm of  $(V^{(N)})^{-1}$  is bounded by

$$\|(V^{(N)})^{-1}\|_2 = \sup_{f^{(N)} \neq 0} \left\{ \frac{\|(V^{(N)})^{-1} f^{(N)}\|_2}{\|f^{(N)}\|_2} \right\} = \sup_{f^{(N)} \neq 0} \left\{ \frac{\|a^{(N)}\|_2}{\|f^{(N)}\|_2} \right\} \leq \rho_*^N \Lambda_N. \quad (32)$$

■

Note that the bound above applies to any simply connected compact domain  $\Omega \subset \mathbb{C}$  that contains the set of interpolation points  $Z$ .

**Observation 2.5.** In the case where the set of  $(N+1)$  interpolation points  $Z \subset \Omega$  are chosen such that the associated Lebesgue constant  $\Lambda_N \lesssim 1$ , we observe in practice that the upper bound  $\rho_*^N \Lambda_N$  is close to the value of  $\|(V^{(N)})^{-1}\|_2$  (see Figures 10 and 14 for numerical evidence).

**Remark 2.6.** A worst case upper bound for  $\|a^{(N)}\|_2$  is provided by inequality (31) in the proof of Theorem 2.5, as the right-hand side of this inequality depends only on the size of  $F$ .

**Remark 2.7.** Formula (4.5) in [7] establishes the bound  $\|(V^{(N)})^{-1}\|_\infty \leq \Delta_N(D_1, \Omega) \cdot \Lambda_N$ , where  $\Delta_N(D_1, \Omega) := \sup_{p \in \mathcal{P}_N, p \neq 0} \frac{\|p\|_{L^\infty(D_1)}}{\|p\|_{L^\infty(\Omega)}}$ , and  $\mathcal{P}_N$  denotes the set of all polynomials of degree less than or equal to  $N$ . By combining the maximum principle with Lemma 2.3, we obtain the bound  $\Delta_N(D_1, \Omega) \leq \rho_*^N$ , from which it follows that  $\|(V^{(N)})^{-1}\|_\infty \leq \rho_*^N \Lambda_N$ . This result can alternatively be obtained more directly using the inequality

$$\|(V^{(N)})^{-1}\|_\infty = \sup_{f^{(N)} \neq 0} \left\{ \frac{\|a^{(N)}\|_\infty}{\|f^{(N)}\|_\infty} \right\} \leq \sup_{f^{(N)} \neq 0} \left\{ \frac{\|a^{(N)}\|_2}{\|f^{(N)}\|_\infty} \right\} \leq \rho_*^N \Lambda_N, \quad (33)$$

where the final inequality follows from (31).

## 2.1 Under what conditions is interpolation in the monomial basis as good as interpolation in a well-conditioned polynomial basis?

As before, we assume that the simply connected compact set  $\Omega$  is inside the unit disk centered at the origin (such that  $\gamma_N \lesssim 1$ ). Furthermore, we choose a set of  $(N+1)$

interpolation points  $Z \subset \Omega$  with a Lebesgue constant  $\Lambda_N \lesssim 1$ , and let  $V^{(N)}$  denote the corresponding Vandermonde matrix. Recall from Theorem 2.2 that, if

$$\|(V^{(N)})^{-1}\|_2 \leq \frac{1}{2u \cdot \gamma_N}, \quad (34)$$

then the monomial approximation error  $\|F - \widehat{P}_N\|_{L^\infty(\Omega)}$  is bounded a priori by

$$\|F - \widehat{P}_N\|_{L^\infty(\Omega)} \lesssim \|F - P_N\|_{L^\infty(\Omega)} + u \cdot \|a^{(N)}\|_2, \quad (35)$$

where  $u$  denotes machine epsilon,  $\widehat{P}_N$  is the computed monomial expansion,  $P_N$  is the exact  $N$ th degree interpolating polynomial of  $F$  for the set of interpolation points  $Z$ , and  $a^{(N)}$  is the monomial coefficient vector of  $P_N$ .

By Theorem 2.4, if we choose a constant  $C_N \geq 0$  and a finite sequence of polynomials  $\{Q_n\}_{n=0,1,\dots,N}$  such that  $\|F - Q_n\|_{L^\infty(\Omega)} \leq C_N \rho_*^{-n}$  for  $0 \leq n \leq N$ , where  $Q_n$  has degree  $n$  and  $\rho_*$  is given in Definition 2.2, then the monomial coefficient vector  $a^{(N)}$  of  $P_N$  satisfies

$$\|a^{(N)}\|_2 \lesssim C_N \Lambda_N N \approx C_N, \quad (36)$$

and inequality (35) becomes

$$\|F - \widehat{P}_N\|_{L^\infty(\Omega)} \lesssim \|F - P_N\|_{L^\infty(\Omega)} + u \cdot C_N. \quad (37)$$

In practice, one can take  $\{Q_n\}_{n=0,1,\dots,N}$  to be a finite sequence of interpolating polynomials  $\{P_n\}_{n=0,1,\dots,N}$  of  $F$  for sets of interpolation points with Lebesgue constants  $\lesssim 1$ . When the Lebesgue constant  $\Lambda_N$  is small, it follows from Theorem 2.5 that the condition (34) is satisfied when  $\rho_*^N \lesssim \frac{1}{u}$ . Suppose, then, that  $N$  is sufficiently small so that  $\rho_*^N \lesssim \frac{1}{u}$ . Without loss of generality, we assume that the upper bound for  $\|F - P_n\|_{L^\infty(\Omega)}$ , i.e.,  $C_N \rho_*^{-n}$ , is tight, in the sense that there exists some integer  $n \in [0, N]$  such that  $\|F - P_n\|_{L^\infty(\Omega)} = C_N \rho_*^{-n}$ . Note that the smallest uniform approximation error we can hope to obtain in practice is  $u \cdot \|F\|_{L^\infty(\Omega)}$ .

When  $u \cdot C_N \lesssim \max(\|F - P_N\|_{L^\infty(\Omega)}, u \cdot \|F\|_{L^\infty(\Omega)})$ , the use of a monomial basis for interpolation introduces essentially no extra error. Interestingly, this happens both if the polynomial interpolation error decays quickly and if the polynomial interpolation error decays slowly. Suppose that the polynomial interpolation error decays quickly, so that the bound is tight for  $n = 0$ , i.e.,  $\|F - P_0\|_{L^\infty(\Omega)} = C_N$ . Since  $C_N \lesssim 2\|F\|_{L^\infty(\Omega)}$ , we see that the extra error caused by the use of a monomial basis is bounded by  $u \cdot C_N \lesssim 2u \cdot \|F\|_{L^\infty(\Omega)} \lesssim u \cdot \|F\|_{L^\infty(\Omega)}$ . Examples of this situation are illustrated in Figure 7. Alternatively, suppose that the polynomial interpolation error decays slowly, so that bound is tight for  $n = N$ , i.e.,  $\|F - P_N\|_{L^\infty(\Omega)} = C_N \rho_*^{-N}$ . Since we assumed that  $\rho_*^N \lesssim \frac{1}{u}$ , it follows that  $u \cdot C_N \lesssim \|F - P_N\|_{L^\infty(\Omega)}$ . Examples of this situation are illustrated in Figure 8.

When  $u \cdot C_N \gtrsim \max(\|F - P_N\|_{L^\infty(\Omega)}, u \cdot \|F\|_{L^\infty(\Omega)})$ , stagnation of convergence can occur. In practice, we observe that the extra error caused by the use of the monomial basis, i.e.,  $u \cdot \|a^{(N)}\|_2$ , is close to  $u \cdot C_N$ , so the monomial approximation error  $\|F - \widehat{P}_N\|_{L^\infty(\Omega)}$  generally stagnates at an error level around  $u \cdot C_N$ . Note that a slow decay in  $\|F - P_n\|_{L^\infty(\Omega)}$  results in a larger value of  $C_N$ , while a fast decay in  $\|F - P_n\|_{L^\infty(\Omega)}$  favors a smaller final interpolation error  $\|F - P_N\|_{L^\infty(\Omega)}$ . This means that, for stagnation of convergence to occur, the polynomial interpolation error has to

exhibit some combination of slow decay followed by fast decay. Furthermore, note that an upper bound for  $C_N$  is given by  $C_N \lesssim \rho_*^N$  (see Remark 2.6). This means that, the smaller the value of  $N$ , the smaller the maximum possible value of  $C_N$ , and the more rapid the rate of decay in  $\|F - P_n\|_{L^\infty(\Omega)}$  required for stagnation of convergence to occur. We present examples of this situation in Figure 9.

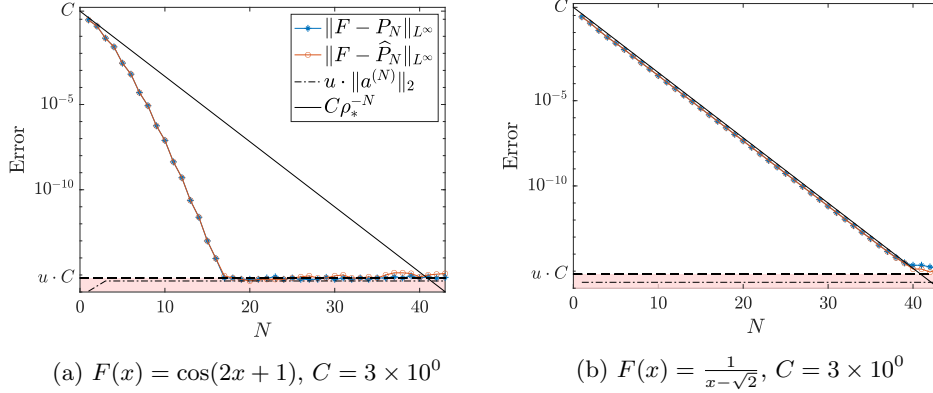


Figure 7: **Cases when the extra error caused by the use of a monomial basis is negligible.** The function  $F$  is interpolated over  $\Omega = [-1, 1]$ . The value of  $C$  is chosen such that  $\|F - P_N\|_{L^\infty([-1,1])} \leq C\rho_*^{-N}$  for  $N = 0, 1, \dots, 40$ . We highlight the region bounded above by  $u \cdot C$  in pink.

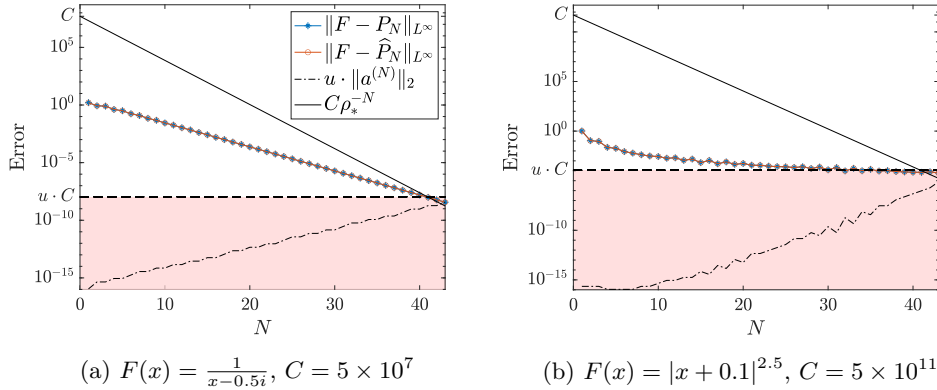


Figure 8: **Cases when the extra error caused by the use of a monomial basis is no larger than  $\|F - P_N\|_{L^\infty(\Omega)}$ .** The function  $F$  is interpolated over  $\Omega = [-1, 1]$ . The value of  $C$  is chosen such that  $\|F - P_N\|_{L^\infty([-1,1])} \leq C\rho_*^{-N}$  for  $N = 0, 1, \dots, 40$ . We highlight the region bounded above by  $u \cdot C$  in pink.

## 2.2 Practical use of a monomial basis for interpolation

What are the restrictions on polynomial interpolation in the monomial basis? Firstly, extremely high-order global interpolation is impossible in the monomial basis, because the order  $N$  must satisfy  $\|(V^{(N)})^{-1}\|_2 \lesssim \frac{1}{u}$  for our estimates to hold, where  $u$  denotes



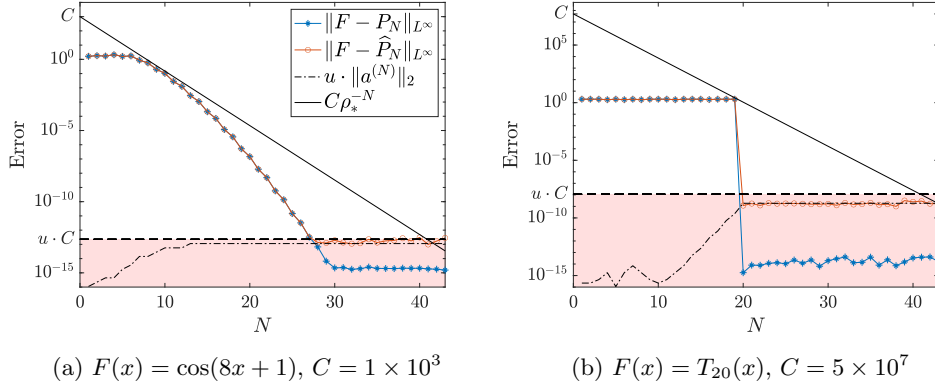


Figure 9: **Cases when convergence stagnates.** The function  $F$  is interpolated over  $\Omega = [-1, 1]$ . The value of  $C$  is chosen such that  $\|F - P_N\|_{L^\infty([-1,1])} \leq C\rho_*^{-N}$  for  $N = 0, 1, \dots, 40$ . We highlight the region bounded above by  $u \cdot C$  in pink.

machine epsilon. In fact, even if this condition were not required, there would still be no benefit in taking an order larger than this threshold. For most functions, if a polynomial of degree exceeding the threshold is needed to resolve the function to machine precision, the error caused by the use of a monomial basis typically dominates the true polynomial interpolation error, which leads to stagnation of convergence. This can be seen from the discussion in Section 2.1.

On the other hand, piecewise polynomial interpolation in the monomial basis over a partition of  $\Omega$  can be carried out stably, provided that the maximum order of approximation over each subelement of  $\Omega$  is maintained below the threshold  $\arg \max_N \|(V^{(N)})^{-1}\|_2 \lesssim \frac{1}{u}$ , and that the size of  $u \cdot \|a^{(N)}\|_2 \approx u \cdot \|\hat{a}^{(N)}\|_2$  is kept below the size of the polynomial interpolation error, where  $a^{(N)}$  and  $\hat{a}^{(N)}$  denote the exact and the computed monomial coefficient vectors, respectively. As demonstrated in Section 2.1, the latter requirement is often satisfied automatically, and when it is not, adding an extra level of subdivision almost always resolves the issue. In addition, the extra error caused by the use of a monomial basis can always be estimated promptly during computation, using the value of  $u \cdot \|\hat{a}^{(N)}\|_2$ .

Based on the discussion above, we summarize a proper method of using the monomial basis for interpolation, as follows. For simplicity, we use the same order of approximation over each subelement, and denote the order by  $N$ . This value of  $N$  needs to be smaller than the threshold  $\arg \max_N \|(V^{(N)})^{-1}\|_2 \lesssim \frac{1}{u}$ . Given a function  $F : \Omega \rightarrow \mathbb{C}$  and an error tolerance  $\varepsilon$ , we subdivide the domain  $\Omega$  until  $F$  can be approximated by a polynomial of degree less than or equal to  $N$  over each subelement to within an error of  $\varepsilon$ . Finally, we subdivide the subelements further until the 2-norm of the monomial coefficient vector  $\hat{a}^{(N)}$  is less than  $\varepsilon/u$  over each subelement.

Since the convergence rate of piecewise polynomial approximation is  $\mathcal{O}(h^{N+1})$ , where  $h$  and  $N$  denote the maximum diameter and minimum order of approximation over all subelements, respectively, and since the aforementioned threshold is generally not small (e.g., the threshold is approximately equal to 43 when  $\Omega = [-1, 1]$ ), piecewise polynomial interpolation in the monomial basis converges rapidly so long as we set the value of  $N$  to be large enough. Therefore, there is no need to avoid the use of a monomial basis when it offers an advantage over other bases.

**Remark 2.8.** It takes  $\mathcal{O}(N^3)$  operations to solve a Vandermonde system of size  $N \times N$  by a standard backward stable solver. Since the order of approximation  $N$  is almost always not large, the solution to the Vandermonde system can be computed both rapidly, as well as accurately in the sense that  $\gamma_N$  is small, using highly optimized linear algebra libraries, e.g., LAPACK. There also exist specialized algorithms that solve Vandermonde systems in  $\mathcal{O}(N^2)$  operations, e.g., the Björck-Pereyra algorithm [10] and the Parker-Traub algorithm [16]. We note that the Parker-Traub algorithm is known to be backward stable [16], while the stability of the Björck-Pereyra algorithm is known only under very restrictive conditions [20].

### 3 Numerical experiments

#### 3.1 Interpolation over an interval

In this section, we consider polynomial interpolation in the monomial basis over an interval  $\Omega = [a, b] \subset \mathbb{R}$ . We compute the polynomial interpolants using Chebyshev points on the interval  $[a, b]$ , since their associated Lebesgue constant,  $\Lambda_N$ , is bounded by  $\frac{2}{\pi} \log(N + 1) + 1$ , where  $N$  is the order of approximation [12].

In Figure 10, we report the values of  $\|(V^{(N)})^{-1}\|_2$  and its upper bound  $\rho_*^N \Lambda_N$  (see Theorem 2.5), for the domains  $\Omega = [-1, 1]$  and  $\Omega = [0, 1]$ . One can see that the upper bound is close to being tight. Note that when  $\Omega = [-1, 1]$ , we have that  $\rho_* = 1 + \sqrt{2}$  and  $\|(V^{(N)})^{-1}\|_2 \leq \frac{1}{u}$  for  $N \leq 43$ ; when  $\Omega = [0, 1]$ , we have that  $\rho_* = 3 + 2\sqrt{2}$  and  $\|(V^{(N)})^{-1}\|_2 \leq \frac{1}{u}$  for  $N \leq 22$ .

In Figure 11, we interpolate several functions over  $\Omega = [-1, 1]$ . We denote the interpolant constructed using the monomial basis by  $\widehat{P}_N$ , and estimate the true polynomial interpolant  $P_N$  using the Lagrange basis evaluated by the Barycentric interpolation formula. In addition to the estimated values of  $\|F - P_N\|_{L^\infty([-1, 1])}$  and  $\|F - \widehat{P}_N\|_{L^\infty([-1, 1])}$ , we plot three additional curves in each figure: the estimated values of  $u \cdot \|a^{(N)}\|_2$  based on inequality (15), the upper bound  $C\rho_*^{-N}$  for  $\|F - P_N\|_{L^\infty([-1, 1])}$ , where  $C$  was chosen so that  $\|F - P_N\|_{L^\infty([-1, 1])} \leq C\rho_*^{-N}$  for  $N = 0, 1, \dots, 40$ , and the approximate upper bound  $u \cdot C$  for  $u \cdot \|a^{(N)}\|_2$ . In Figure 12, we provide similar experiments for the case where  $\Omega = [0, 1]$ , this time choosing  $C$  so that  $\|F - P_N\|_{L^\infty([0, 1])} \leq C\rho_*^{-N}$  for  $N = 0, 1, \dots, 20$ . Based on these experimental results, one can observe that the convergence stagnates after the monomial approximation error  $\|F - \widehat{P}_N\|_{L^\infty(\Omega)}$  reaches  $u \cdot \|a^{(N)}\|_2$ , which implies that inequality (35) is sharp. Moreover, the values of  $u \cdot \|a^{(N)}\|_2$  are always less than the upper bound  $u \cdot C$ , which agrees with our analysis in Section 2.1.

What happens when the order of approximation  $N$  exceeds the threshold, i.e., when  $\|(V^{(N)})^{-1}\|_2 \geq \frac{1}{u}$ ? In Figure 13, we use two different solvers to solve the Vandermonde system with Chebyshev interpolation points over the interval  $[-1, 1]$ : LU factorization with partial pivoting, and the truncated singular value decomposition (TSVD) with a truncation cutoff of  $10^{-14}$ . Since backward stability no longer guarantees that  $\|\widehat{a}^{(N)}\|_2 \approx \|a^{(N)}\|_2$  when  $N$  is greater than the threshold, the upper bound for the monomial approximation error (16) becomes invalid, and our previous analysis is no longer applicable. As shown in the experiments, the approximation error does not improve when  $N > 43$ . When the system is solved using LU decomposition, the error fluctuates. We also note that the error could grow exponentially after  $N$  exceeds the threshold, depending on the particular choice of the backward stable solver. When

the TSVD is used, the error is stable. This can be explained by Theorem 2.1 in [37], which provides an analogous bound to (16) for the case of the TSVD.

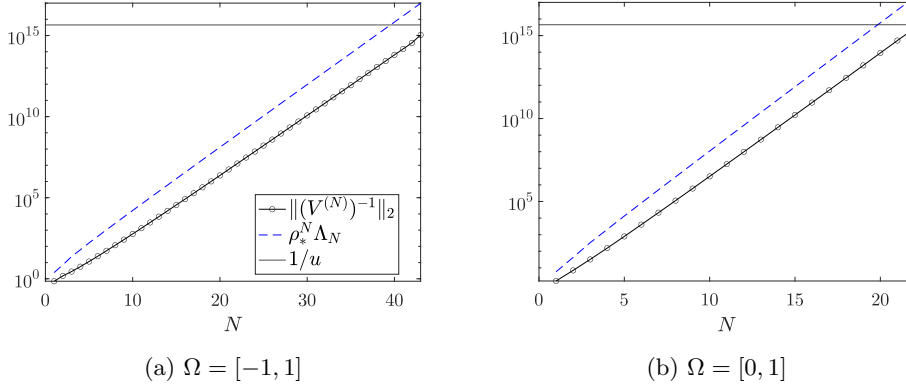


Figure 10: **The 2-norm of  $(V^{(N)})^{-1}$  with Chebyshev interpolation points over an interval  $\Omega$ , and its upper bound, for different orders of approximation.** We note that  $\rho_* = 1 + \sqrt{2}$  when  $\Omega = [-1, 1]$ , and  $\rho_* = 3 + 2\sqrt{2}$  when  $\Omega = [0, 1]$ .

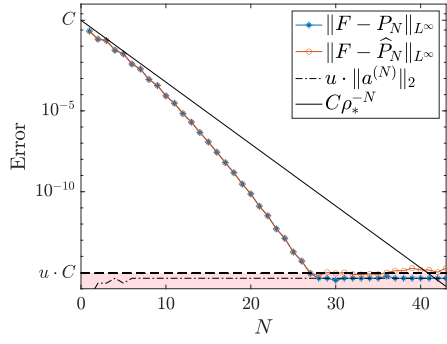
### 3.2 Approximation over more general regions in the complex plane

In this section, we consider polynomial interpolation and approximation in the monomial basis over a more general simply connected compact set  $\Omega \subset \mathbb{C}$ . When  $\partial\Omega$  is an analytic Jordan curve, it is shown in [28] that the Lebesgue constant of the Fejér points  $\{\Phi^{-1}(\exp(i(\frac{2\pi j}{N+1} + a)))\}_{j=0,1,\dots,N}$  grows logarithmically, where  $\Phi^{-1}$  is defined in Remark 2.3, and where  $a \in \mathbb{R}$  is arbitrary. When  $\Omega$  is a Jordan arc, it is shown in [38] that the Lebesgue constant of the Fejér points, with some adjustment to ensure adequate spacing between interpolation points, also exhibits logarithmic growth.

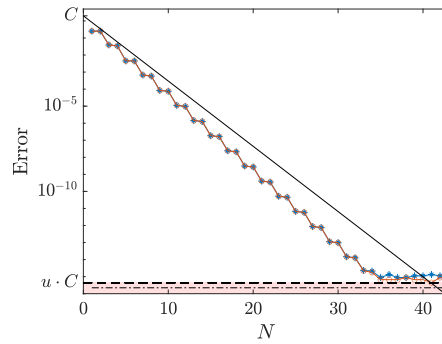
In the remainder of this section, we provide several numerical experiments involving the following three domains: an ellipse with a major radius of 1 and a minor radius of 0.2, centered at the origin (see Figure 6d); a parabola parameterized by  $g : [-1, 1] \rightarrow \mathbb{C}$ , where  $g(t) := t + 0.4i(t^2 - 1)$  (see Figure 6e); and a square with side length  $\sqrt{2}$ , centered at the origin. We note that the estimated constants  $\rho_*$  (see Definition 2.2) for the three domains are approximately 2, 2.6, and 1.3, respectively (see Figures 6d, 6e, and 6f).

In the first domain (the ellipse), the conformal mapping  $\Phi^{-1}$  is specified by the formula  $\Phi^{-1}(z) = \frac{3}{5} \cdot z + \frac{2}{5} \cdot \frac{1}{z}$ , and we use the Fejér points for interpolation. Since the Fejér points for the second and the third domains are not known in closed form, we employ different approaches tailored to each case. In the second domain (the parabola), we set the interpolation points to be  $\{g(t_j)\}_{j=0,1,\dots,N}$ , where  $\{t_j\}_{j=0,1,\dots,N}$  is the set of  $(N+1)$  Chebyshev points on the interval  $[-1, 1]$ . We find that the Lebesgue constants associated with these points are all less than 10 when  $\kappa(V^{(N)}) \lesssim \frac{1}{u}$ . In the third domain (the square), we instead solve a least-squares fitting problem with sampling points chosen to be the  $2(N+1)$  Chebyshev points of the first kind along each side of the square, where  $N$  denotes the order of approximation (see Remark 2.2).

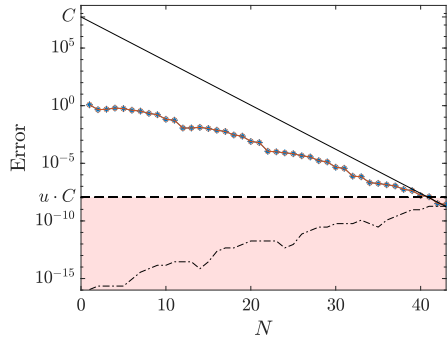
In Figure 14, we report the values of  $\|(V^{(N)})^{-1}\|_2$  and its upper bound  $\rho_*^N \Lambda_N$  (see Theorem 2.5) for the ellipse domain and the parabola domain, where the value of  $\rho_*$



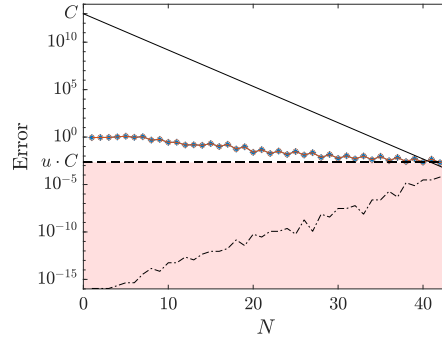
(a)  $F(x) = e^{-2(x+0.1)^2}$ ,  $C = 4 \times 10^0$



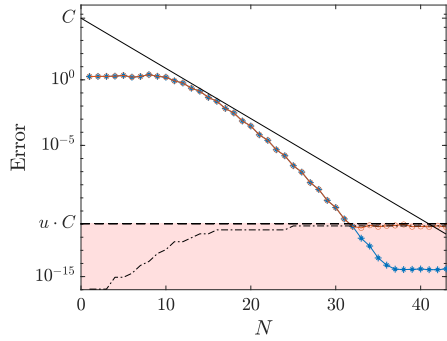
(b)  $F(x) = \tan(x)$ ,  $C = 2 \times 10^0$



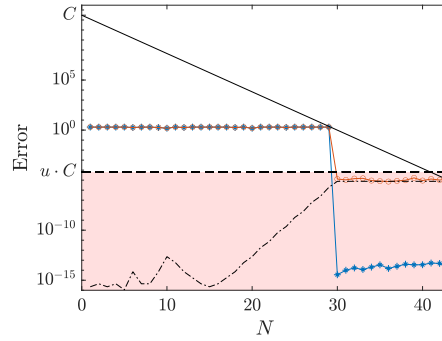
(c)  $F(x) = \cos(3x^8 + 1)$ ,  $C = 5 \times 10^7$



(d)  $F(x) = |\sin(5x)|^3$ ,  $C = 1 \times 10^{13}$

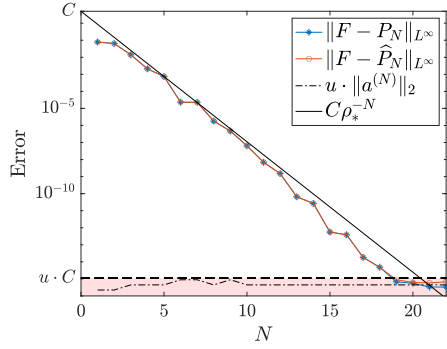


(e)  $F(x) = \cos(12x + 1)$ ,  $C = 5 \times 10^4$

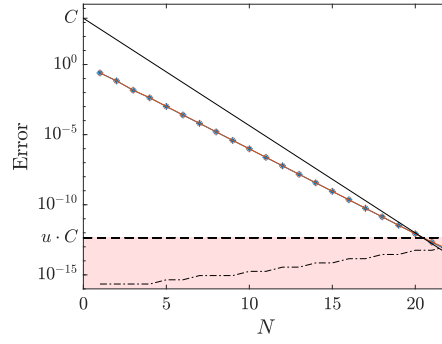


(f)  $F(x) = T_{30}(x)$ ,  $C = 3 \times 10^{11}$

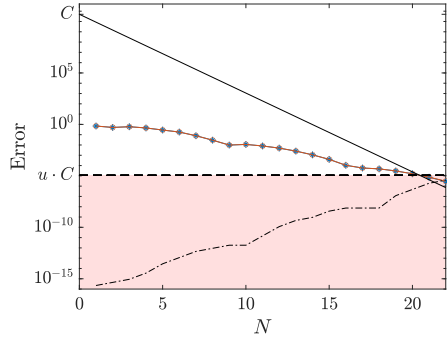
Figure 11: **Polynomial interpolation in the monomial basis over  $\Omega = [-1, 1]$ .** The constant  $\rho_*$  equals  $1 + \sqrt{2}$ . The value of  $C$  is chosen such that  $\|F - P_N\|_{L^\infty([-1,1])} \leq C\rho_*^{-N}$  for  $N = 0, 1, \dots, 40$ . We highlight the region bounded above by  $u \cdot C$  in pink.



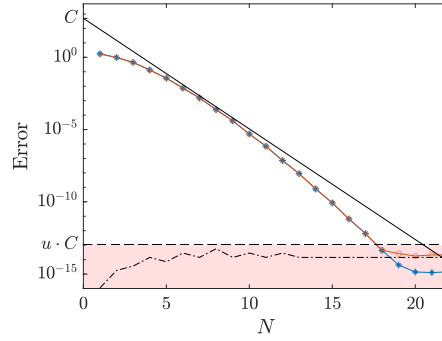
(a)  $F(x) = e^{-2(x+0.1)^2}$ ,  $C = 5 \times 10^0$



(b)  $F(x) = \tan(x)$ ,  $C = 2 \times 10^3$

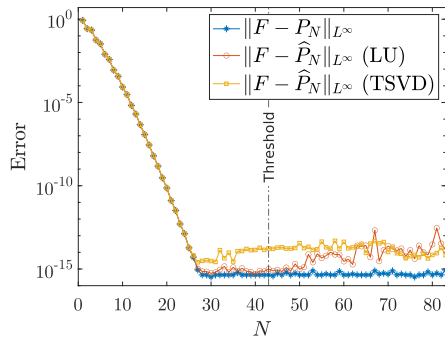


(c)  $F(x) = \cos(3x^8 + 1)$ ,  $C = 5 \times 10^{10}$

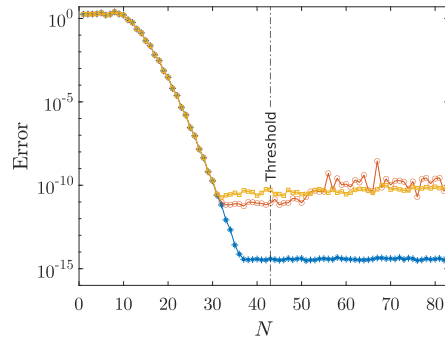


(d)  $F(x) = \sin(6x + 1)$ ,  $C = 5 \times 10^2$

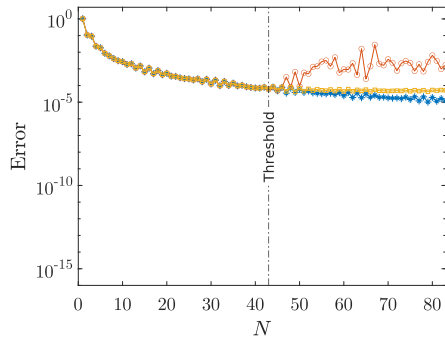
Figure 12: **Polynomial interpolation in the monomial basis over  $\Omega = [0, 1]$ .** The constant  $\rho_*$  equals  $3 + 2\sqrt{2}$ . The value of  $C$  is chosen such that  $\|F - P_N\|_{L^\infty([0,1])} \leq C\rho_*^{-N}$  for  $N = 0, 1, \dots, 20$ . We highlight the region bounded above by  $u \cdot C$  in pink.



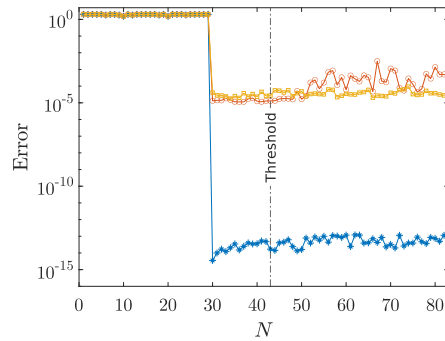
(a)  $F(x) = e^{-2(x+0.1)^2}$



(b)  $F(x) = \cos(12x + 1)$

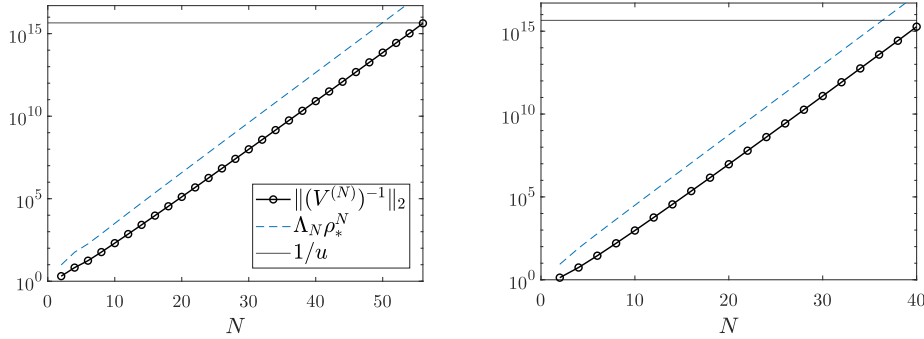


(c)  $F(x) = |x + 0.1|^{2.5}$



(d)  $F(x) = T_{30}(x)$

Figure 13: **Polynomial interpolation in the monomial basis over  $\Omega = [-1, 1]$ , when the order of approximation exceeds the threshold.** The vertical line with the label ‘Threshold’ denotes the order of approximation  $\min(\{N : \|(V^{(N)})^{-1}\|_2 \geq \frac{1}{u}\})$ , beyond which our theory is no longer applicable.



(a) The ellipse,  $\rho_* \approx 2$

(b) The parabola,  $\rho_* \approx 2.6$

Figure 14: **The 2-norm of  $(V^{(N)})^{-1}$  and its upper bound.**

for each domain is estimated based on the plots in Figure 6. Again, one can see that our upper bound is very tight.

In Figures 15, 16, and 17, we report the estimated values of  $\|F - P_N\|_{L^\infty(\Omega)}$ ,  $\|F - \hat{P}_N\|_{L^\infty(\Omega)}$ , and  $u \cdot \|a^{(N)}\|_2$ , over each of these three domains. We estimate the exact polynomial interpolant  $P_N$  by expressing  $P_N$  in a discrete orthogonal polynomial basis (which is well-conditioned), computed using the Vandermonde with Arnoldi orthogonalization procedure [11]. In addition, we report the the upper bound  $C\rho_*^{-N}$  for  $\|F - P_N\|_{L^\infty(\Omega)}$ , where  $C$  is chosen so that  $\|F - P_N\|_{L^\infty(\Omega)} \leq C\rho_*^{-N}$  for a range of  $N$  indicated in the figure caption, and the upper bound  $u \cdot C$  for  $u \cdot \|a^{(N)}\|_2$ . These results demonstrate that the observations made at the near end of Section 3.1 are indeed applicable to more general domains in the complex plane, and to polynomial approximation using least-squares fitting with monomials.

**Remark 3.1.** In certain applications [18, 2, 29], the function  $F : \Gamma \rightarrow \mathbb{C}$  is defined by the formula  $F(z) := \sigma(g^{-1}(z))$ , where  $\Gamma$  is a simple smooth arc,  $g : [-1, 1] \rightarrow \mathbb{C}$  is an analytic function that parameterizes  $\Gamma$ , and  $\sigma : [-1, 1] \rightarrow \mathbb{C}$  is analytic. In this case, the analytic continuation of  $F$  can have a singularity close to  $\Gamma$  even when  $\sigma$  is entire, because the inverse of the parameterization (i.e.,  $g^{-1}$ ) has so-called Schwarz singularities at  $z = g(t^*)$ , where  $g'(t^*) = 0$ . In [2], the authors show that, the higher the curvature of the arc  $\Gamma$ , the closer the singularity induced by  $g^{-1}$  is to  $\Gamma$ . As a result, the approximation of such a function  $F$  by polynomials is efficient only when the curvature of  $\Gamma$  is small.

## 4 Applications

After justifying the use of a monomial basis for polynomial interpolation, a natural question to ask is why one would want to use it in the first place. For one, the monomial basis is the simplest polynomial basis to manipulate. For example, the evaluation of an  $N$ th degree polynomial expressed in the monomial basis can be achieved using only  $N$  multiplications through the application of Horner's rule. This evaluation can be further accelerated using Estrin's scheme [13], which leverages instruction-level parallelism in modern CPUs. This type of parallelism is typically unavailable when evaluating a polynomial expressed in an orthogonal polynomial basis.

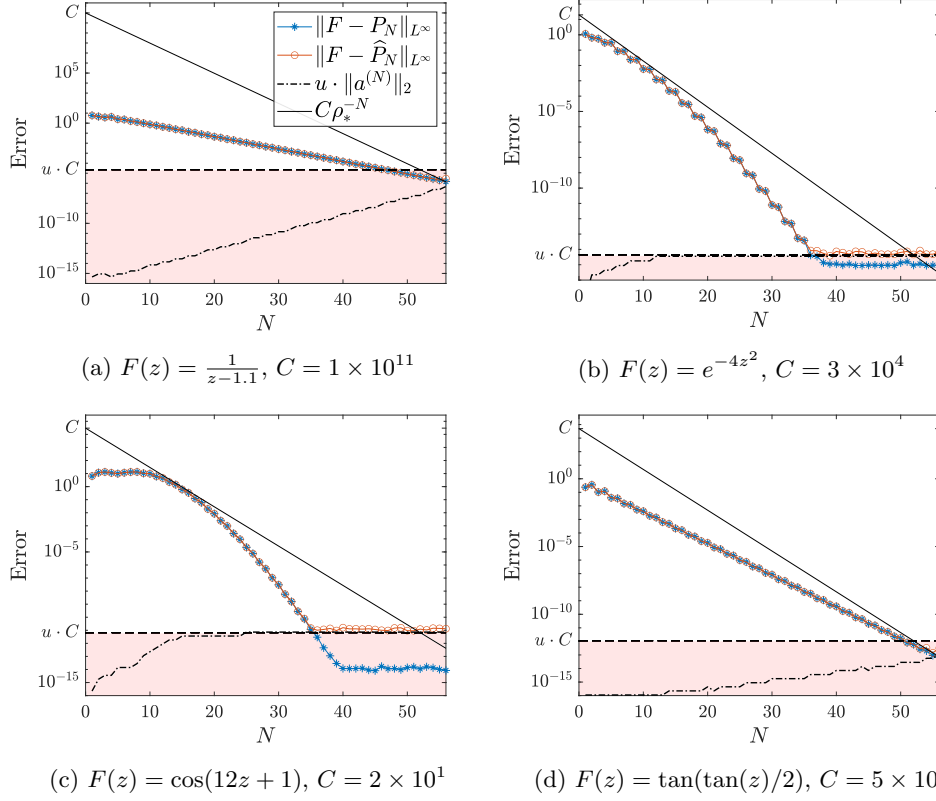


Figure 15: **Polynomial interpolation in the monomial basis over the ellipse  $\Omega$ .** We estimate  $P_N$  by expressing it in a discrete orthogonal polynomial basis, computed using the Vandermonde with Arnoldi orthogonalization procedure [11]. The constant  $\rho_*$  is approximately equal to 2.0. The value of  $C$  is chosen such that  $\|F - P_N\|_{L^\infty(\Omega)} \leq C\rho_*^{-N}$  for  $N = 0, 1, \dots, 55$ . We highlight the region bounded above by  $u \cdot C$  in pink.



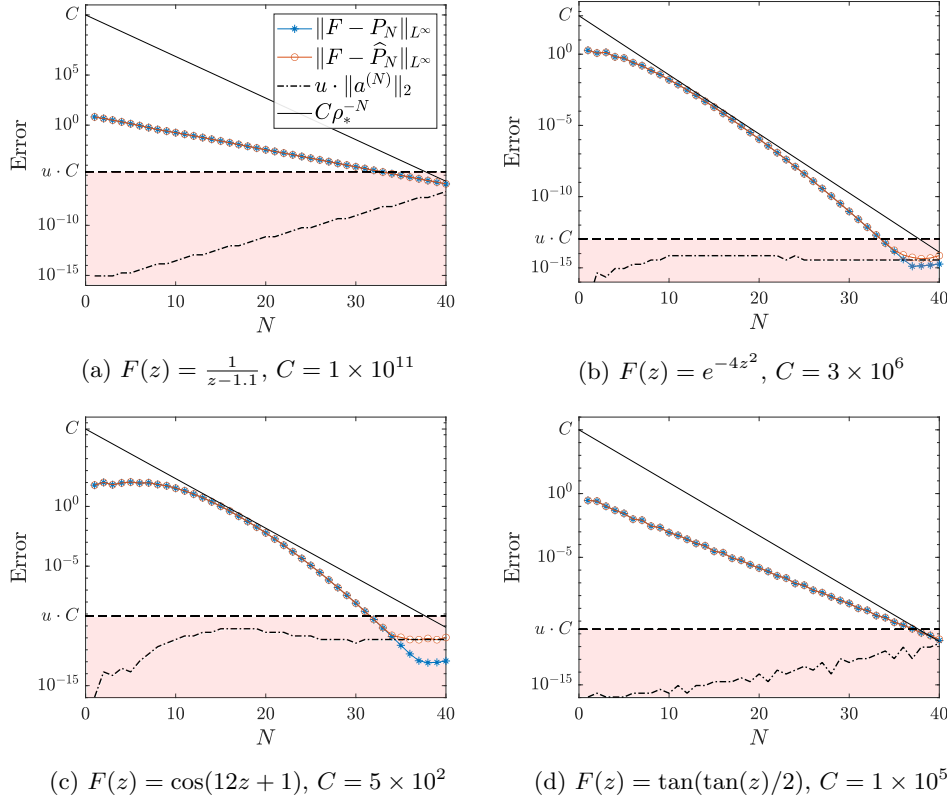


Figure 16: **Polynomial interpolation in the monomial basis over the parabola  $\Omega$ .** We estimate  $P_N$  by expressing it in a discrete orthogonal polynomial basis, computed using the Vandermonde with Arnoldi orthogonalization procedure [11]. The constant  $\rho_*$  is approximately equal to 2.6. The value of  $C$  is chosen such that  $\|F - P_N\|_{L^\infty(\Omega)} \leq C\rho_*^{-N}$  for  $N = 0, 1, \dots, 40$ . We highlight the region bounded above by  $u \cdot C$  in pink.

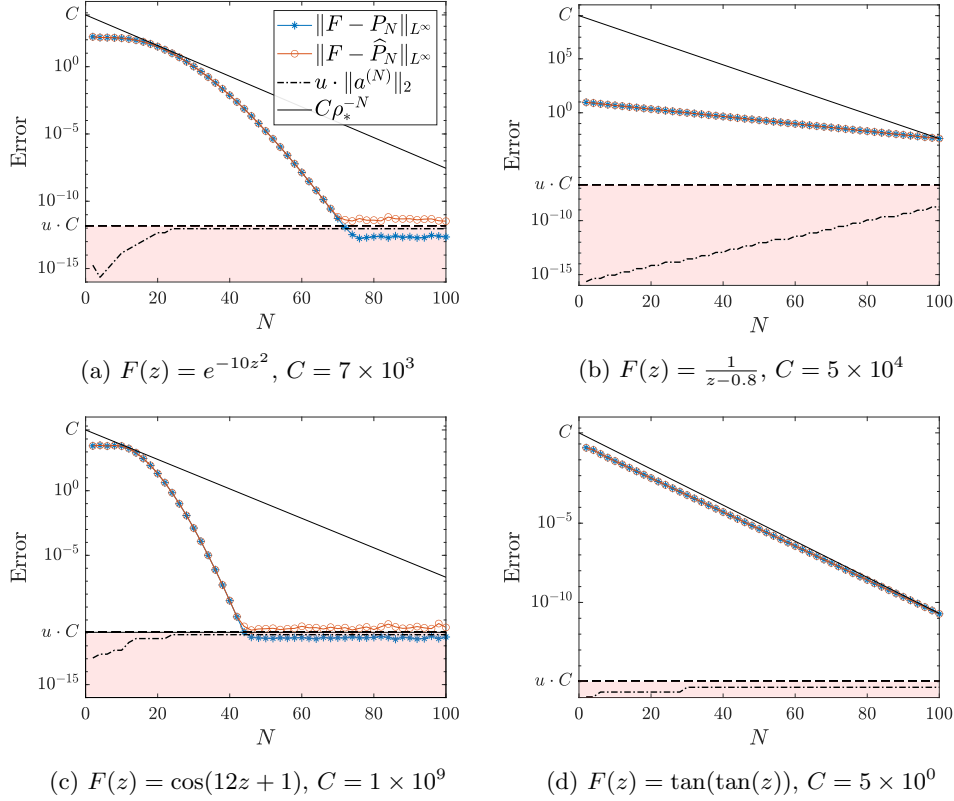


Figure 17: **Polynomial approximation in the monomial basis over the square  $\Omega$ .** We estimate  $P_N$  by expressing it in a discrete orthogonal polynomial basis, computed using the Vandermonde with Arnoldi orthogonalization procedure [11]. The constant  $\rho_*$  is approximately equal to 1.3 (see Figure 6f). The value of  $C$  is chosen such that  $\|F - P_N\|_{L^\infty(\Omega)} \leq C\rho_*^{-N}$  for  $N = 0, 1, \dots, 100$ . We highlight the region bounded above by  $u \cdot C$  in pink.

Besides this obvious advantage, we discuss some other applications below.

## 4.1 Oscillatory integrals and singular integrals

Given an oscillatory or singular function  $\Psi : \Gamma \rightarrow \mathbb{C}$  and a smooth function  $F : \Gamma \rightarrow \mathbb{C}$  over a smooth simple arc  $\Gamma \subset \mathbb{C}$ , the calculation of  $\int_{\Gamma} \Psi(z)F(z) dz$  by standard quadrature rules can be extremely expensive or inaccurate due to the oscillations or the singularity of  $\Psi$ . However, when  $F$  is a monomial, there exists a wide range of integrals in this form that can be efficiently computed to high accuracy by either analytical formulas or by recurrence relations, often derived using integration by parts. Therefore, when the smooth function  $F$  is accurately approximated by a monomial expansion of order  $N$ , such integrals can be efficiently evaluated by the formula  $\sum_{k=0}^N a_k \left( \int_{\Gamma} \Psi(z)z^k dz \right)$ , where  $\{a_k\}_{k=0,1,\dots,N}$  denotes the coefficients of the monomial expansion. Integrals of this type include the Fourier integral  $\int_a^b e^{icx} F(x) dx$  and various layer potentials and Stieltjes transforms, e.g.,  $\int_{\Gamma} \log(z-\xi)F(z) dz$  and  $\int_{\Gamma} \frac{F(z)}{z-\xi} dz$ , where  $\xi \in \mathbb{C}$  is given. We refer the readers to [23, 24] for more detailed discussion on the Fourier integral, and to [18, 2, 29] for more detailed discussion on the application of polynomial interpolation in the monomial basis to the evaluation of layer potentials. Some interesting applications can also be found in [19, 1, 25].

## 4.2 Root finding

Given a simply connected compact set  $\Omega \subset \mathbb{C}$  and a function  $F : \Omega \rightarrow \mathbb{C}$ , one method for computing the roots of  $F$  over  $\Omega$  is to first approximate  $F$  by a polynomial  $P_N(z) = \sum_{j=0}^N a_j z^j$  to high accuracy, and then to compute the roots of  $P_N$  by calculating the eigenvalues of the corresponding companion matrix, which we denote by  $C(P_N)$ . Recently, a backward stable algorithm that computes the eigenvalues of  $C(P_N)$  in  $\mathcal{O}(N^2)$  operations with  $\mathcal{O}(N)$  storage has been proposed in [5]. This algorithm is backward stable in the sense that the computed roots are the exact roots of a perturbed polynomial  $\hat{P}_N(z) = \sum_{j=0}^N (a_j + \delta a_j) z^j$ , so that the backward error satisfies  $\|\delta a^{(N)}\|_2 \lesssim u \|a^{(N)}\|_2$ , where  $u$  denotes machine epsilon,  $\delta a^{(N)} := (\delta a_0, \delta a_1, \dots, \delta a_N)^T$  and  $a^{(N)} := (a_0, a_1, \dots, a_N)^T$ . It follows that  $\|P_N - \hat{P}_N\|_{L^\infty(\Omega)} \leq \|\delta a^{(N)}\|_1 \lesssim u\sqrt{N+1} \|a^{(N)}\|_2$ . When  $\|a^{(N)}\|_2 \approx \|P_N\|_{L^\infty(\Omega)}$ , the computed roots are backward stable in the polynomial  $P_N$ . This condition, however, does not hold for all polynomials  $P_N$ . Furthermore, the calculation of the coefficients  $a^{(N)}$  from the function  $F$ , which involves the solution of a Vandermonde system of equations, is highly ill-conditioned. In this paper, we show that, when  $F$  is sufficiently smooth (in the mild sense discussed in Section 2.1), it is possible to compute the coefficients of an interpolating polynomial  $P_N(z) = \sum_{j=0}^N a_j z^j$ , with  $\|a^{(N)}\|_2 \approx \|F\|_{L^\infty(\Omega)}$ , which approximates  $F$  uniformly to high accuracy, even when the condition number of the Vandermonde matrix is close to the reciprocal of machine epsilon. From this, we see that a backward stable root finder can be constructed by combining the piecewise polynomial approximation procedure described in Section 2.2 with the algorithm presented in [5]. Interestingly, by using the least-squares fitting procedure described in Section 3.2 for the case when  $\Omega$  is a square, an adaptive root-finding algorithm for a complex analytic function in a square domain, analogous to the one described in [36], can be developed utilizing solely the monomial basis.

## 5 Discussion

Since the invention of digital computers, most research on the topic of polynomial interpolation in the monomial basis has focused on showing that it is a bad idea. The condition number of Vandermonde matrices has been studied extensively in recent decades (see [15] for a literature review), and it is known that its growth rate is at least exponential, unless the interpolation points are asymptotically distributed uniformly on the complex unit circle centered at the origin [26]. As a result, the computed monomial coefficients are generally highly inaccurate when the dimensionality of the Vandermonde matrix is not small. For this reason, other better-conditioned bases are often used for polynomial interpolation [32, 11]. On the other hand, it has long been observed that polynomial interpolation in the monomial basis produces highly accurate approximations for many smooth functions (see, for example, [17, 18]). This is because computing the monomial coefficients inaccurately does not imply that the resulting interpolating polynomial is necessarily a poor approximation, since it is the backward error  $\|V^{(N)}\hat{a}^{(N)} - f^{(N)}\|_2$  of the numerical solution  $\hat{a}^{(N)}$  to the Vandermonde system  $V^{(N)}a^{(N)} = f^{(N)}$  that determines the approximation accuracy, and  $\|V^{(N)}\hat{a}^{(N)} - f^{(N)}\|_2$  can be small even when the condition number  $\kappa(V^{(N)})$  is large. It is easy to show that  $\|V^{(N)}\hat{a}^{(N)} - f^{(N)}\|_2 \lesssim u \cdot \|a^{(N)}\|_2$ , where  $u$  denotes machine epsilon, from which one can show that the monomial approximation error is bounded by the sum of the polynomial interpolation error and the extra error term  $u \cdot \|a^{(N)}\|_2$ . In this paper, we establish an upper bound for  $\|a^{(N)}\|_2$  that depends on the polynomial interpolation errors  $\{\|F - P_n\|_{L^\infty}\}_{n=0,1,\dots,N}$ . Based on this bound, we find that this extra error term is generally smaller than the polynomial interpolation error, provided that the order of approximation is no larger than the maximum order allowed by the constraint  $\kappa(V^{(N)}) \lesssim \frac{1}{u}$  (see Section 2.1). This finding elucidates the unexpectedly good performance of polynomial interpolation using the monomial basis in practical applications. In the rare situations where the monomial basis results in a less accurate interpolant, we show that such instances can be easily identified and corrected a posteriori, leading to a robust algorithm for piecewise polynomial interpolation over simply connected compact regions in the complex plane using the monomial basis, with no extra error and with almost no extra cost (see Section 2.2). As a by-product of our analysis, we derive a tight upper bound for the condition number of any Vandermonde matrix (see Theorem 2.5), which includes several previously established results [14, 15] as special cases. Finally, we present applications where using the monomial basis for interpolation is particularly advantageous (see Section 4).

While not discussed in this paper, our results can be easily generalized to higher dimensions and to polynomial approximants constructed using least-square fitting. In [30], we study bivariate polynomial interpolation in the monomial basis over a (possibly curved) triangle, and demonstrate that similarly accurate approximations can be constructed for orders up to 20, regardless of the triangle's aspect ratio.

## 6 Acknowledgements

We are deeply grateful to James Bremer, Daan Huybrechs, Andreas Klöeckner, Adam Morgan, Nick Trefethen, and the anonymous referees for their valuable advice and insightful discussions.

## References

- [1] af Klinteberg, L., Askham, T., Kropinski, M. C.: A Fast Integral Equation Method for the Two-Dimensional Navier-Stokes Equations. *J. Comput. Phys.*, **409**, 109353 (2020)
- [2] af Klinteberg, L., Barnett, A. H.: Accurate Quadrature of Nearly Singular Line Integrals in Two and Three Dimensions by Singularity Swapping. *BIT Numer. Math.* **61.1**, 83–118 (2021)
- [3] Adcock, B., Huybrechs, D.: Frames and Numerical Approximation. *SIAM Rev.* **61**(3), 443–473 (2019)
- [4] Adcock, B., Huybrechs, D.: Frames and Numerical Approximation II: Generalized Sampling. *J. Fourier Anal. Appl.* **26**(6), 1–34 (2020)
- [5] Aurentz, J. L., Mach, T., Vandebril, R., Watkins, D. S.: Fast and Backward Stable Computation of Roots of Polynomials. *SIAM J. Matrix Anal. Appl.* **36**(3), 942–973 (2015)
- [6] Barnett, A. H., Betcke, T.: Stability and Convergence of the Method of Fundamental Solutions for Helmholtz Problems on Analytic Domains. *J. Comput. Phys.* **227**(14), 7003–7026 (2008)
- [7] Beckermann, B.: On the numerical condition of polynomial bases: estimates for the condition number of Vandermonde, Krylov and Hankel matrices. PhD dissertation, Verlag nicht ermittelbar (1997)
- [8] Beckermann, B.: The Condition Number of Real Vandermonde, Krylov and Positive Definite Hankel Matrices. *Numer. Math.* **85**(4), 553–577 (2000)
- [9] Berrut, J.-P., Trefethen, L. N.: Barycentric Lagrange Interpolation. *SIAM Rev.* **46**(3), 501–517 (2004)
- [10] Björck, Å., Pereyra, V.: Solution of Vandermonde Systems of Equations. *Math. Comput.* **24**(112), 893–903 (1970)
- [11] Brubeck, P. D., Nakatsukasa Y., Trefethen, L. N.: Vandermonde with Arnoldi, *SIAM Rev.* **63**(2), 405–415 (2021)
- [12] Ehlich, H., Zeller, K.: Auswertung der Normen von Interpolationsoperatoren. *Math. Ann.* **164**, 105–112 (1966)
- [13] Estrin, G.: Organization of Computer Systems: The Fixed plus Variable Structure Computer. *Proc. Western Joint Computer Conference*, 33–40 (1960)
- [14] Gautschi, W.: The Condition of Polynomials in Power Form. *Math. Comput.* **33**(145), 343–352 (1979)
- [15] Gautschi, W.: How (Un)stable are Vandermonde Systems?. *Asymptot. Comput. Anal.* **124**, 193–210 (1990)
- [16] Gohberg, I., Olshevsky, V.: The Fast Generalized Parker-Traub Algorithm for Inversion of Vandermonde and Related Matrices. *J. Complex.* **13**(2), 208–234 (1997)

- [17] Heath, M. T.: *Scientific Computing: An Introductory Survey*, Revised Second Edition. SIAM (2018)
- [18] Helsing, J., Ojala, R.: On the Evaluation of Layer Potentials Close to Their Sources. *J. Comput. Phys.* **227**(5), 2899–2921 (2008)
- [19] Helsing, J., Jiang, S.: On Integral Equation Methods for the First Dirichlet Problem of the Biharmonic and Modified Biharmonic Equations in NonSmooth Domains. *SIAM J. Sci. Comput.* **40**(4), A2609–2630 (2018)
- [20] Higham, N. J.: Error Analysis of the Björck-Pereyra Algorithms for Solving Vandermonde Systems, *Numer. Math.* 50.5, 613–632 (1987).
- [21] Higham, N. J.: *Accuracy and Stability of Numerical Algorithms*, SIAM (2002).
- [22] Higham, N. J.: The Numerical Stability of Barycentric Lagrange Interpolation. *IMA J. Numer. Anal.* **24**(4), 547–556 (2004)
- [23] Iserles, A., Nørsett, S. P.: Efficient Quadrature of Highly Oscillatory Integrals Using Derivatives. *Proc. Math. Phys. Eng.* **461**(2057), 1383–1399 (2005)
- [24] Iserles, A., Nørsett, S. P., Olver, S.: Highly Oscillatory Quadrature: The Story So Far. In: *Proceedings of ENUMATH, Santiago de Compostela (2006)*. Springer, Berlin, 97–118 (2006)
- [25] Ojala, R., Tornberg, A.-K.: An Accurate Integral Equation Method for Simulating Multi-Phase Stokes Flow. *J. Comp. Phys.* **298**, 145–160 (2015)
- [26] Pan, V. Y.: How Bad are Vandermonde Matrices?. *SIAM J. Matrix Anal. Appl.* **37**(2), 676–694 (2016)
- [27] Pommerenke, C.: *Boundary Behaviour of Conformal Maps*. Vol. 299. Springer Science & Business Media (2013).
- [28] Reichel, L.: On Polynomial Approximation in the Complex Plane with Application to Conformal Mapping. *Math. Comput.*, **44**(170), 425–433 (1985).
- [29] Wu, B., Zhu, H., Barnett, A., Veerapaneni S.: Solution of Stokes Flow in Complex Nonsmooth 2D Geometries via a Linear-Scaling High-Order Adaptive Integral Equation Scheme. *J. Comput. Phys.* **410**, pp. 109361 (2020)
- [30] Shen, Z, Serkh, K.: Rapid Evaluation of Newtonian Potentials on Planar Domains. *SIAM J. Sci. Comput.* **46**(1), A609–628 (2024)
- [31] Stein, D. B., Barnett, A. H.: Quadrature by Fundamental Solutions: Kernel-Independent Layer Potential Evaluation for Large Collections of Simple Objects. *Adv. Comput. Math.* **48**(60) (2022)
- [32] Trefethen, L. N.: *Approximation Theory and Approximation Practice*. SIAM (2019)
- [33] Trefethen, L. N.: Polynomial and Rational Convergence Rates for Laplace Problems on Planar Domains. *Proc. Roy. Soc. A*, **480**(2295) (2024)
- [34] Trefethen, L. N., Bau, D.: *Numerical Linear Algebra*. SIAM (1997)

- [35] Walsh, J. L.: Interpolation and Approximation by Rational Functions in the Complex Domain. vol. 20. AMS, Philadelphia (1935)
- [36] Zhang, H., Rokhlin V.: Finding Roots of Complex Analytic Functions via Generalized Colleague Matrices. *Adv. Comput. Math.* **50**(4), 71 (2024)
- [37] Zhao, M, Serkh, K.: On the Approximation of Singular Functions by Series of Non-integer Powers. arXiv:2308.10439v2 (2023)
- [38] Zhong, L. F., Zhu, L. Y.: The Marcinkiewicz-Zygmund Inequality on a Smooth Simple Arc. *J. Approx. Theory* **83**(1), 65–83 (1995)